

Time-dependent diffusion of Cosmic Rays from discrete sources: I- Method and analytical solutions

R. Taillet^{1,2}

P. Salati^{1,2}, D. Maurin^{3,4}

E. Vangioni-Flam³ and M. Cassé^{3,4}

¹ *Laboratoire de Physique Théorique LAPTH, Annecy-le-Vieux, 74941, France*

² *Université de Savoie, Chambéry, 73011, France*

³ *Institut d'Astrophysique de Paris, 98 bis Bd Arago, 75014 Paris, France*

⁴ *SAP, CEA, Orme des Merisiers, 91191 Gif-sur-Yvette, France*

Received December 12, 2018; accepted

ABSTRACT

The current progress in our understanding of cosmic ray physics (acceleration, propagation) points towards the necessity to go beyond the steady-state hypothesis. For several problems related to cosmic rays nuclei, the effect of nearby and/or recent sources may be great enough to make a more precise description mandatory. It is all the more true given the precision of present and future space missions (e.g. INTEGRAL, AMS, AGILE, GLAST). More precisely, the goal of modelling individual nearby sources becomes within reach. Propagation from these sources to the Solar neighborhood requires to carefully take into account the effect of escape, galactic wind and spallations. To this aim, this paper proposes an exact analytic solution to the time-dependent diffusion equation when these effects are taken into account with the same modelling as in our previous studies with a continuous source distribution, for which an extensive set of results are available. As a by-product, we derive an alternative description of the steady-state model which has a better convergence and is thus best suited for point sources than the usual Bessel-Fourier expansion. To get some insight on the effect of the source discreteness on the cosmic ray composition, we also compare the path-length distribution for a set of discrete sources and for a continuous source distribution. Our conclusions disagree with those of Higdon and Lingelfelter (2003). The case of a linear wind is compared to the case of a constant wind

presenting a discontinuity through the galactic disk, and a useful correspondence between the two situations is presented. This paper is essentially thought of as a toolbox, the study of the physical consequences of the results presented here being currently investigated and postponed to a future work.

Subject headings: Cosmic rays

1. Introduction

The cosmic ray flux at any given position in the Galaxy is due to many sources, which are probably somehow related to the remnants of supernovae. Given the time and space scales relevant to this problem, the sources can be considered as point sources emitting a puff of cosmic rays during a short time. Each source of position \vec{r}_i and age t_i yields, at position \vec{r}_0 and time $t = 0$ (now), a flux $N(\vec{r}_i, t_i, \vec{r}_0, t_0 = 0)$ that can be obtained by solving the diffusion equation with the appropriate source term and boundary conditions (see below). The total flux is given by

$$\mathcal{N}(\vec{r}_0) = \sum_i N(\vec{r}_i, t_i, \vec{r}_0) . \quad (1)$$

This model has been coined Myriad model by Higdon and Lingenfelter (2003). Most studies assume that this sum may be approximated by an integral

$$\mathcal{N}(\vec{r}_0) \approx \int d^2\vec{r} \int dt N(\vec{r}, t, \vec{r}_0) , \quad (2)$$

which is equivalent in the limit of a source distribution which is continuous in space and time (continuous distributions for \vec{r}_i and t_i). This approximation is justified if the sources are numerous and densely distributed, but it probably fails for nearby and/or recent sources, for which the detailed location and age should be known. This is particularly true for species that have a short propagation range, such as high energy electrons (their range is limited by energy losses) or radioactive species having a lifetime of the order of 1 Myr (see Donato et al. (2002) for a discussion on the role of the local environment, such as the local bubble, on these species).

One can find in the literature several analytical formulae extracted from various propagation models to study cosmic ray charged nuclei. As regards the spatial “discreteness”, Lezniak and Webber (1979) start with the time dependent solution when both spallations and energy losses are taken into account, to eventually derive the steady-state Green function necessary to study the no near source effect (expected to reproduce the depletion at low grammage for the path length distribution). From what concerns the temporal “discreteness”, in the

framework of halo models, Owens (1976) derived time dependent solutions (see also Lezniak (1979)), including spallations but assuming a gaz density which is constant throughout the diffusive volume (in this case the mean time and the mean matter crossed are proportional). The most complete work to provide “simple” formula to the time-dependent case is probably Freedman et al. (1980). These authors derive the mean age and the grammage distribution to seek if it is possible to constrain the propagation parameters from current observations of charged nuclei. They conclude that a large degeneracy in propagation parameters remain in most cases. Finally, further formulae including energy losses have been provided in Lerche and Schlickeiser (1982), but due to the generality of the treatment they are a bit too complicated for our purpose. All these studies deal with GeV charged nuclei *here* and *now*. It has been shown that the high energy electron and positrons are particularly sensitive to nearby sources, due to their huge energy losses (Aharonian et al. (1995), see also Coswik and Lee (1979)). A nearby source such as the SNR associated with the Geminga pulsars probably has a great influence on them. The situation is less clear about the stable charged cosmic ray spectra, but nearby sources are expected to be more and more important as energy grows. Whereas some authors estimate the contribution from Geminga to be at most 10% (Johnson (1994)), some others (Erlykin and Wolfendale (2001a)) argue that a single supernova evenement can explain the feature observed in the spectrum at a few PeV. This could be the Sco-Cen association that is expected to be the only possible one able to generate the Local Bubble 11 Myr ago (Benítez et al. (2002)). Anisotropy provides an additional test to this hypothesis. (see e.g. Dorman et al. (1985)). It can also be further checked by gathering observations from the past and from the rest of the Galaxy. For instance, Ramadurai (1993) argued that Geminga could be responsible for an increase of the Cosmic ray flux by a factor 1.8 by inspection of Antarctic ice sediments. The measurement of the isotopic composition of the Earth crust (see e.g. Knie et al. (1999)), of meteorites, and of ice cores may be used to investigate the time variation of the cosmic ray flux on Earth (see also Erlykin and Wolfendale (2001b)). It has been proposed that the observed variations could be partly due to a single recent supernovae (Fields and Ellis (1999)). Shaviv (2002) has even studied the passage through arms and connection with ice ages. Anyway, one can finally use the information carried by GeV photons from the entire Galaxy to see how they are produced considering a discret model for sources.

The aim of this paper is to provide convenient formulae to be able to deal with many of the above questions (this will be achieved in the companion paper). For that purpose, we use a model that is a natural extension of the stationnary propagation model we have used in previous studies. We first investigate in Sec. 2 results from the steady-state limit, to comment about spatial discretness. The path-length distribution, which gives an indication on the elemental composition of cosmic rays, is derived and compared to a recent study. It

has been claimed by Higdon and Ligenfelter (2003) that the Myriad model yields a strong deviation of the path-length distribution compared to the Leaky Box case. We argued that the method used by these authors is not correct. We present the results obtained by an analytical solution of the propagation equation, taking into account the possibility that these Cosmic Rays may be blown away by a convective wind, as suggested by magneto-hydrodynamical studies and observations of galaxies. As the use of linear and constant wind are sometimes disputed in the literature, we show that they lead to exactly the same path-length distribution and thus both descriptions are related (as long as energy losses are discarded). Then we proceed to the full time dependent solution in Sec. 3. Taken in the limit of stationary sources, it provides an alternative formulation of the stationary solution (that presents a very good convergence). Finally, we very briefly introduce a criterium to classify nearby/recent sources in a $(r, \sqrt{2Kt})$ plane. We then conclude. For the sake of compactness and clarity, the derivation of several expressions have been postponed to the Appendix.

2. Steady-state path-length distribution from a generalized diffusion equation

In this section, we investigate the effect of the source discreteness on the chemical composition of Cosmic Rays, using the path-length distribution, the definition of which we first remind.

2.1. Definitions – Generalized diffusion equation

Cosmic Rays, during their journey between a source and Earth, cross regions in which interstellar matter is present. This leads to spallations and thus to a change in the chemical composition. A powerful tool to study the spallation-induced change of composition is provided by the path-length distribution, which we now introduce. As a first step, let us assume that Cosmic Rays do not interact with the matter they cross, i.e. the spallations are switched off. These Cosmic Rays can be sorted according to the *grammage*, i.e. the column density of matter they have crossed (usually expressed in g cm^{-2}). We denote $\mathcal{N}(\vec{r}_s, \vec{r}_o, x)$ the density of Cosmic Rays originating from a source located at \vec{r}_s , detected at \vec{r}_o , and having crossed the grammage x . This quantity is called the *path-length distribution*. This quantity has been widely used as i) it isolates the propagation properties from the nuclear aspects and ii) this quantity may be investigated experimentally without prior knowledge of the details of the propagation model. It provides a tool to compare the Cosmic Ray composition from several diffusion models, as similar path-length distributions give rise to similar compositions

(see Secs. 2.4 and 2.5)

The total density, when spallations are switched off, is given by

$$N(\vec{r}_s, \vec{r}_o, \sigma = 0) = \int_0^\infty \mathcal{N}(\vec{r}_s, \vec{r}_o, x) dx . \quad (3)$$

Now, spallations have a destructive effect, and a primary cosmic ray having crossed a gram-mage x has a survival probability given by $\exp(-\sigma x/m)$, which depends on the cross section σ . In the following, m will denote the *mean* mass of the interstellar medium atoms. The probability for a Cosmic Ray emitted in \vec{r}_s and reaching \vec{r}_o to travel unharmed can thus be written as

$$\mathcal{P}(\vec{r}_s, \vec{r}_o) = \int_0^\infty \mathcal{P}(\text{survive}|x) \times \mathcal{P}(x|\vec{r}_s, \vec{r}_o) dx . \quad (4)$$

This becomes inexact when energy losses are considered. In that case, as the survival probability depends on the energy of the Cosmic Ray when it crosses the disk, the previous equation would read for an infinitely thin matter disk

$$\begin{aligned} \mathcal{P}(\vec{r}_s, \vec{r}_o) = & \int_0^\infty dx \{ \mathcal{P}(x, E_1, E_2, \dots, E_x | \vec{r}_s, \vec{r}_o) \\ & \times \int_0^\infty \mathcal{P}(\text{survive}|E_1) \int_0^\infty \mathcal{P}(\text{survive}|E_2) \dots \int_0^\infty \mathcal{P}(\text{survive}|E_x) \} , \end{aligned} \quad (5)$$

where E_i is the energy at the i -th crossing, $\mathcal{P}(\text{survive}|E_i)$ is the probability to survive a crossing at energy E_i and $\mathcal{P}(x, E_1, E_2, \dots, E_x | \vec{r}_s, \vec{r}_o)$ is the probability that the x crossings occur at the respective energies E_1, \dots, E_n . This gives a hint to why the weighted slab approach is much more cumbersome to use when energy variations are considered (see e.g. Stephens and Streitmatter (1998) for an illustration).

When energy losses are discarded, Eq. (4) leads to a generalization of expression (3),

$$N(\vec{r}_s, \vec{r}_o, \sigma) = \int_0^\infty \exp\left\{-\frac{\sigma}{m}x\right\} \mathcal{N}(\vec{r}_s, \vec{r}_o, x) dx .$$

The density, as a function of σ/m , is thus given by the Laplace transform of the path-length distribution. One way to determine the path-length distribution is to first compute the quantity $N(\vec{r}_s, \vec{r}_o, \sigma)$ for any value of σ , by solving the propagation equation, and try to invert the relation (2.1). Unfortunately, there is no general procedure to perform this inversion, even numerically. A noticeable exception is the Leaky Box, for which

$$N(\sigma) \propto \frac{1}{1 + \lambda_e \sigma/m} \quad \text{and} \quad \mathcal{N}(x) \propto \exp(-x/\lambda_e) .$$

In Sec. 2.4, we give the path-length distribution for point sources in our particular diffusion model. This distribution will be expressed as an infinite sum of Leaky Boxes. Path-length distributions corresponding to several other models can be found in Margolis (1986).

We follow another approach to determine the path-length distribution, inspired by Jones (1979). It consists in writing a generalized diffusion equation, describing the evolution of $\mathcal{N}(\vec{r}, t, x)$ which gives, at time t and location \vec{r} , the density of particles which have crossed a grammage x , when the destructive effect of spallations is *not* taken into account. This approach is related to the weighted slab, as the path-length distribution will be used to infer the density of particles having survived spallations. This generalized equation is easily obtained for a primary as

$$\frac{\partial \mathcal{N}(\vec{r}, t, x)}{\partial t} = K \Delta \mathcal{N}(\vec{r}, t, x) + q(\vec{r}, t) \delta(x) - \frac{\partial \mathcal{N}(\vec{r}, t, x)}{\partial x} m v n_{\text{ism}}(\vec{r}), \quad (6)$$

where in the right-hand side, the first term stands for diffusion, the second is the source term (creating particles with zero grammage) and the third gives the evolution of the grammage when matter is present, and using

$$\left. \frac{\partial \mathcal{N}(\vec{r}, t, x)}{\partial t} \right|_{\text{gram}} = - \frac{\partial \mathcal{N}(\vec{r}, t, x)}{\partial x} m v n_{\text{ism}}(\vec{r}). \quad (7)$$

It should be noted that when the density n_{ism} is not homogeneous in the whole diffusive volume, grammage is not proportional to time (this will be discussed further in Sec. 2.3).

This equation can be compared to the usual diffusion equation describing the evolution of $N(\vec{r}, t)$

$$\frac{\partial N(\vec{r}, t)}{\partial t} = K \Delta N(\vec{r}, t) + q(\vec{r}, t) - \sigma m v n_{\text{ism}}(\vec{r}) N(\vec{r}, t).$$

We emphasize that Eq. (6) does not take into account the influence of the spallations on propagation, but rather introduces the variable x as a counter which keep tracks of the quantity of matter crossed by the Cosmic Rays, spallations being switched off. We solve this equation in two cases: i) continuous sources in a non homogeneous spallative disk, to discuss Higdon's results, and 2) a point source in a homogeneous disk, to be used in the Myriad model.

2.2. Application to diffusion in a non homogeneous thin disk

We now solve Eq. (6) in the case under study, for the steady-state case

$$0 = K \left\{ \frac{1}{r} \frac{\partial}{\partial r} \left(r \frac{\partial \mathcal{N}(r, z, x)}{\partial r} \right) + \frac{\partial^2 \mathcal{N}(r, z, x)}{\partial z^2} \right\} - V_c \frac{\partial \mathcal{N}(r, z, x)}{\partial z}$$

$$+q(r)\delta(z)\delta(x) - \frac{\partial \mathcal{N}(r, z, x)}{\partial x} m v \Sigma_{\text{ism}}^0 f(r) \delta(z), \quad (8)$$

with $f(r) \equiv \Sigma(r)/\Sigma_{\text{ism}}^0$ and $\Sigma_{\text{ism}}^0 \equiv 6.2 \times 10^{20} \text{ cm}^{-2}$ (Ferrière (1998)) is the local surface density of the galactic disk. Performing Fourier-Bessel transforms using the J_0 functions

$$\mathcal{N}(r, z, x) = \sum_{i=0}^{\infty} \mathcal{N}_i(z, x) J_0 \left(\zeta_i \frac{r}{R} \right),$$

one finds (see Appendix B for details)

$$\mathcal{N}_i(0, x) = \sum_{j=0}^{\infty} a_{ij} e^{-x/x_j} \Theta(x), \quad (9)$$

where $\Theta(x)$ is the Heavyside distribution and the x_j are the eigenvalues of the matrix

$$A_{ij} = \frac{m v \Sigma_{\text{ism}}^0}{2K} \left(\frac{1}{r_w} + \frac{S_i}{2} \coth \left(\frac{S_i L}{2} \right) \right)^{-1} \alpha_{ij} \quad \text{with} \quad S_i = 2 \left(\frac{1}{r_w^2} + \frac{\zeta_i^2}{R^2} \right)^{1/2},$$

and where we have introduced the matrix

$$\alpha_{ij} = \frac{2}{J_1^2(\zeta_i)} \int_0^1 \rho J_0(\zeta_i \rho) J_0(\zeta_j \rho) f(\rho r) d\rho.$$

It can be noted that the mean grammage, which happens to be the escape length λ_e introduced in the Leaky Box models, can be expressed as

$$\langle x \rangle = \frac{\sum_i q_i J_0(\zeta_i R_\odot/R) \sum_{j=0}^{\infty} a_{ij} x_j^2}{\sum_i q_i J_0(\zeta_i R_\odot/R) \sum_{j=0}^{\infty} a_{ij} x_j}. \quad (10)$$

2.3. Difficulties with the Higdon and Lingenfelter approach

Another method is proposed in Higdon and Lingenfelter (2003) to compute the path-length distribution from the cosmic ray density due to each discrete source and the matter distribution in the diffusive volume. We believe their approach is not correct. In particular, these authors mix up the grammage as a parameter (independent from t , as in their Eq. 4.3) and its mean value (which does depend on t , as in their Eqs. 4.1 and 4.2). The change in grammage distribution $\mathcal{N}(\vec{r}, x, t)$ over time, at a given position \vec{r} , depends on the local matter density, and their Eq. (4.3) should actually be written as our Eq. (7), i.e. using their notations

$$\frac{\partial \omega(\vec{r}, x, t)}{\partial t} = 1.4 m_H \beta c n_{\text{ism}}(\vec{r}) \frac{\partial \omega(\vec{r}, x, t)}{\partial x}.$$

Using the analytical approach presented above, we compute the path-length distribution for the matter and source distribution used in Higdon and Lingenfelter (2003). Among other things, these authors study the influence of the H_2 distribution, which has the form of a ring located at $r \sim 4$ kpc. They find that this component may lead to a feature in the path-length distribution, at $x \sim 2$ g/cm² (their Fig. 3, which is partly reproduced in our Fig. 1). Our results are displayed in Fig. 1; the analytical treatment, which we claim is more correct, does not yield this feature. The distributions appear to be quite close to exponentials., i.e. to Leaky Box distributions.

2.4. Influence of the spatial discreteness of the source distribution

We now want to investigate the effect of discreteness on the Cosmic Ray composition, through the path-length distribution. We first compute this quantity for a point source, and we then compare the path-length distributions obtained for a set of point sources and an equivalent continuous source distribution. For the sake of simplicity, we focus on the case of a uniform distribution of matter. In this case, $\Sigma(r)$ is constant, i.e. $f(r) = 1$, and $\alpha_{ij} = \delta_{ij}$. This matrix is diagonal, so that the previous computation can be simplified. It is then found that

$$\mathcal{N}_i(z, x) = e^{V_c|z|/2K} \frac{\sinh(S_i(L - |z|)/2)}{\sinh(S_iL/2)} \times \frac{q_i}{v\Sigma_{\text{ism}}^0} \exp(-x/x_i) \Theta(x)$$

with

$$x_i = \frac{mv\Sigma_{\text{ism}}^0}{2K} \left(\frac{1}{r_w} + \frac{S_i}{2} \coth\left(\frac{S_iL}{2}\right) \right)^{-1}.$$

When escape and wind are discarded, $x_i \approx 200\text{g cm}^{-2}/\zeta_i$, so that the high i modes contribute to the low grammages. When spallations are switched on

$$N_i(z) = \frac{\sinh(S_i(L - |z|)/2)}{\sinh(S_iL/2)} \times \frac{q_i}{v\Sigma_{\text{ism}}^0\sigma + V_c + KS_i \coth(S_iL/2)}.$$

This is the usual expression for the steady-state density in the particular diffusion model we consider here as we used in previous studies (see e.g. Maurin et al. (2001)).

The q_i are obtained by Fourier-Bessel transforming the radial source distribution. We first consider a point source located at any position in the disk. The cylindrical symmetry of the problem is now broken, but as the influence of the R boundary is expected to be negligible, we consider that diffusion occurs in an infinite plane, and the origin is set at the position of the source. Summations over Bessel functions become integrals, and the final result is easily obtained, performing the substitution $1/J_1^2(\zeta_i) \rightarrow k\pi R/2$, $\sum_i \rightarrow \int d(Rk/\pi)$

and $\zeta_i/R \rightarrow k$, with $z = 0$,

$$\mathcal{N}(r, z = 0, x) = \frac{1}{v\Sigma_{\text{ism}}^0} \int_0^\infty dk J_0(kr) q(k) \exp\left(-\frac{x}{x(k)}\right) \quad (11)$$

with

$$x(k) = \frac{mv\Sigma_{\text{ism}}^0/2K}{1/r_w + S(k) \coth(S(k)L)}$$

and

$$S(k) = 2 \left(\frac{1}{r_w^2} + k^2 \right)^{1/2}, \quad q(k) = k \int_0^\infty r dr \frac{\delta(r)}{2\pi r} J_0(kr) = \frac{k}{2\pi}.$$

In the case of infinite L and $r_w = 0$, one obtains

$$\mathcal{N}(r, z = 0, x) = \frac{1}{2\pi v\Sigma_{\text{ism}}^0} \int_0^\infty dk k J_0(kr) \exp\left(-\frac{kx}{mv\Sigma_{\text{ism}}^0/K}\right) \quad (12)$$

$$= \frac{1}{4\pi K r} \frac{K^2 x}{mv^2(\Sigma_{\text{ism}}^0)^2 r^2} \left(1 + \frac{x^2 K^2}{r^2 m^2 v^2 (\Sigma_{\text{ism}}^0)^2} \right)^{-3/2} \Theta(x) \quad (13)$$

which is exactly equivalent to the expression obtained in Taillet & Maurin (2003), using a random walk approach.

The path-length distributions are shown in Figs. 2 and 3. The higher grammages, corresponding to longer paths, are more suppressed by escape or wind, than lower grammages. The effect of the convective wind is seen to be similar to that of escape, but quantitatively different at low grammages. To understand this, let us first consider diffusion in free space without wind. Several kinds of paths are responsible for low grammages: short paths, connecting us to a nearby source in the disk, and longer paths that wander in the halo without crossing the disk too much. It happens that the second kind is rather important, which explains why escape from a boundary at $z = \pm L$ (which kills the paths wandering too far in the halo) actually affects the low end of the grammage distribution. When wind is present, the short paths are more important, and the low grammages are less affected.

Even for a point source, the path-lengths are quite broadly distributed around the mean value, as can be seen in Figs. 2 and 3. As a result, the grammage distribution due to a set of discrete sources is smoothed to a great extent, so that it is very unlikely to have physical consequences on the composition of Cosmic Rays on Earth. The contributions from continuous sources distributed in several rings (thin lines) are displayed for $L = 5$ kpc in Fig. 4 and for $r_w = 5$ kpc in Fig. 5,

$$\frac{1}{2\pi v\Sigma_{\text{ism}}^0} \frac{2}{R_{\text{max}}^2 - R_{\text{min}}^2} \int_0^\infty dk \{R_{\text{max}} J_1(kR_{\text{max}}) - R_{\text{min}} J_1(kR_{\text{min}})\} \exp\left(-\frac{x}{x(k)}\right).$$

The effect of discreteness is found to be small for the outer rings. The main effect is that when discrete sources are considered, the very nearby sources necessary to flatten the low end of the distribution are always lacking. This effect has indeed been proposed by Lezniak and Webber (1979) to explain the depletion at low grammages that was thought to be observed, before Webber et al. (1998) proposed a settlement to this particular issue. The total path-length distribution is very close to an exponential, as expected for a homogeneous source distribution in an infinite disk (Jones (1979)).

To conclude on this matter, the effect of discreteness on the composition of cosmic rays should be negligible for sources located beyond $r \sim 1$ kpc, as can be read off Fig. 4 and 5.

2.5. Remark: Constant versus linear galactic wind

The previous results, as well as the results presented in our previous works, rely on the assumption of a constant wind presenting a discontinuity through the galactic disk. To probe the sensitivity of our results to this hypothesis, we consider another model in which the value of $V_c = V_0 z$ varies linearly with z . The calculations are detailed in Appendix C, and the results will be used here without further justification. The path-length distribution reads

$$N(r, z, x) = \sum_i 2hq_i J_0 \left(\zeta_i \frac{r}{R} \right) \exp \left(-\frac{x}{x_i} \right) \Theta(x)$$

with

$$x_i = \frac{mv\Sigma_{\text{ism}}^0 L}{2K} \frac{\phi \left(\frac{3+a_i}{4}, \frac{3}{2}; \frac{V_0 L^2}{2K} \right)}{\phi \left(\frac{1+a_i}{4}, \frac{1}{2}; \frac{V_0 L^2}{2K} \right)}, \quad a_i \equiv \frac{2K}{V_0} \frac{\zeta_i^2}{R^2} + 2.$$

where ϕ is the confluent hypergeometric function, also denoted ${}_1F_1$ or M in the literature. The resulting path-length distribution is shown in Fig. (6) for a linear and a discontinuous wind. It appears that these two situations lead to very similar results, and one can establish a correspondence between the parameters V_c and V_0 of these models (see Fig. 7). It must be noted that the energy losses have not been considered here. Adiabatic losses are associated to the wind gradient, and their effect should be different for the two forms of the galactic wind: in the constant case, they are confined to the disk whereas in the linear case, they are present in the whole diffusive volume.

3. Time-dependent solution of the diffusion equation

3.1. The time-dependent diffusion equation and its solutions

We now turn to the problem of discreteness in time. For that, we must solve the time-dependent diffusion problem for an instantaneous source. The corresponding diffusion equation reads, when spallations and galactic wind are present,

$$\frac{\partial N}{\partial t} = K \left\{ \frac{1}{r} \frac{\partial}{\partial r} \left(r \frac{\partial N}{\partial r} \right) + \frac{\partial^2 N}{\partial z^2} \right\} - V_c \text{sign}(z) \frac{\partial N}{\partial z} - 2h\nu\sigma n_{\text{ism}} \delta(z) N .$$

The diffusion process in the z direction and in the radial direction are independent. As only pure diffusion occurs in the radial direction (the radial boundary is neglected), the density can be written as

$$N(r, z, t) = \frac{1}{4\pi Kt} e^{-r^2/4Kt} N(z, t)$$

where the function $N(z, t)$ satisfies a time dependent diffusion equation along z . It is convenient to introduce two typical lengths $r_s = h\nu\sigma n_{\text{ism}}/K$ and $r_w = V_c/2K$, as in Taillet & Maurin (2003), or alternately their reciprocals k_s and k_w , so that $N(z, t)$ is a solution of

$$\frac{\partial N}{\partial(Kt)} = \frac{\partial^2 N}{\partial z^2} - 2k_w \text{sign}(z) \frac{\partial N}{\partial z} - 2k_s \delta(z) N .$$

For point-like and instantaneous sources, the solutions are (see Appendix A)

$$N(r, z, t) = \frac{1}{4\pi Kt} \exp\left(-\frac{r^2}{4Kt}\right) e^{k_w|z|} \sum_{n=1}^{\infty} C_n^{-1} e^{-(k_n^2 + k_w^2)Kt} \sin\{k_n L\} \sin\{k_n(L - |z|)\}$$

where the discrete set of k_n are the solutions of

$$k_n \cotan(k_n L) = -k_s - k_w \tag{14}$$

and

$$C_n = L - \frac{\sin 2k_n L}{2k_n} = L + \frac{(\sin k_n L)^2}{k_n^2} (k_s + k_w) .$$

In particular, the radial distribution in the disk is given by

$$N(r, z = 0, t) = \frac{1}{4\pi Kt} \exp\left(-\frac{r^2}{4Kt}\right) \sum_{n=1}^{\infty} C_n^{-1} e^{-(k_n^2 + k_w^2)Kt} \sin^2\{k_n L\} .$$

Though it is not immediately apparent in this expression, the spallations *are* taken into account, through the Eq. (14) determining the k_n . Moreover, this expression is more general

than the form that is usually found in the literature, considering only the effects of escape, which is obtained by replacing the right-hand side of Eq. (14) by 0.

This expression can be written as

$$\mathcal{N}(r, z = 0, t) = \frac{1}{(4\pi Kt)^{3/2}} \exp\left(-\frac{r^2}{4Kt}\right) g(t),$$

where g is a function such that $g \leq 1$ and r denotes the Galactocentric radius. The case $g = 1$ corresponds to the pure diffusion case, for which the importance of sources according to their position in the (r, \sqrt{Kt}) plane is illustrated in Fig. 8. The function $g(t)$ gives the correction to the purely diffusive case and takes into account all the relevant physical effects. As such, it depends on the propagation parameters (spallation cross-section, galactic wind, halo height). The importance of these effects is not the same for all the sources, depending on their position in the (r, t) plane. In particular, the old (large t) and remote (large r) sources are more affected by all these effects. For large values of t , $g(t)$ goes rapidly to zero, ensuring the convergence of the integral over time in Eq. (2). It also makes the function of r obtained by this integration decreases faster than $1/r$, thus ensuring the convergence of the second integral.

3.2. Reformulation of the steady-state model

The steady-state regime results from the continuous superposition of solutions for instantaneous sources, so that the corresponding solution is given by

$$N_{\text{stat}}(r, z) = \int_{-\infty}^0 N(r, z, t) dt.$$

The integration yields

$$N_{\text{stat}}(r, z) = \frac{1}{K} \exp(-k_s z) \sum_{n=1}^{\infty} C_n^2 K_0\left(r\sqrt{k_n^2 + k_w^2}\right) \sin(k_n L) \sin\{k_n(L - z)\}$$

where the Bessel function of the third kind K_0 has been introduced. The density in the disk is thus given by

$$N_{\text{stat}}(r, z = 0) = \frac{1}{K} \sum_{n=1}^{\infty} C_n^2 K_0\left(r\sqrt{k_n^2 + k_w^2}\right) \sin^2(k_n L).$$

This expression provides an alternative (but is exactly equivalent) to the usual Fourier Bessel expansion, using the J_0 functions. It is particularly well suited for sources sharply localized in space, as point-like sources, because the functions over which the development is performed do not oscillate. Convergence of the series above is fast. We have checked that this expression is fully consistent with the Fourier-Bessel expansion.

3.3. Relative importance of nearby/recent sources

The relative importance of nearby and recent sources can be estimated from Figs. 9, 10 and 11, which show the regions of the $(r, \sqrt{2Kt})$ plane contributing for a given fraction of the flux observed on Earth. These regions are obtained by determining the iso- N contours delimiting a surface \mathcal{S} such that the integral of $N(r, z = 0, t)$ over this surface contribute to a given fraction of the integral of $N(r, z = 0, t)$ over the whole plane $z = 0$. It can be seen, as emphasized in Taillet and Maurin (2003), that the nearby sources give a significant fraction of the total signal. These figures actually give a finer information, also showing the relative contribution of recent sources. We will further use these iso-contours in the companion paper, to quantify more precisely which real sources should be considered as nearby/recent sources. It will be then possible to flag which of them require a full time-dependent treatment.

4. Conclusion and summary

We have investigated the effect of the source discreteness on the Cosmic-Ray composition through their path-length distribution. It appears that except for the sources located very near (closer than about 1 kpc), this effect is very small. We have also taken advantage of our analytic study to show that the effect of the interstellar density inhomogeneity across the disk, as implied by the presence of a H_2 ring, on the path-length distribution is not as important as claimed by Higdon and Lingenfelter (2003). The path-length distribution has been obtained for a constant galactic wind V_c (with a discontinuity through the galactic disk) as well as for a wind varying linearly with z , i.e. $V = V_0 z$. It was found that one can establish an approximate correspondence between these two situations, provided that the respective parameters respect the relation shown in Fig. 7.

It is thus with some confidence that we use the hypothesis of a constant galactic wind to compute the time-dependent Cosmic-Ray density in the presence of wind, spallations and escape. We have derived an analytical expression that takes into account the effect of escape, galactic wind and spallation in a thin disk. This will be used in a future study to model the cosmic ray density on Earth due to a set of discrete sources, some of which are known with some precision. One of the interests of this study is that it will be possible to compare the results from the usual continuous source distribution, for which an extensive set of results are available, to a more realistic discrete distribution, all the effects related to propagation (escape, wind, spallation) being modelled exactly the same way.

Acknowledgments

This work has benefited from the support of PICS 1076, CNRS and of the PNC (Programme National de Cosmologie).

A. Time dependent solution of the diffusion equation

A.1. The time-dependent diffusion equation

The cosmic-ray density N follows the time-dependent diffusion equation

$$\frac{\partial N}{\partial t} + \vec{\nabla} \cdot \left\{ -K \vec{\nabla} N + N \vec{V}_c \right\} = -v \sigma_{\text{ism}} \delta(z) N , \quad (\text{A1})$$

where both disk spallations and galactic wind have been taken into account. The convection velocity \vec{V}_c lies in the vertical direction and drags the particles outside so that its value is given by $\text{sign}(z) V_c$ where a constant value for V_c has been assumed. That relation may be written as

$$\frac{\partial N}{\partial t} = K \left\{ \frac{1}{r} \frac{\partial}{\partial r} \left(r \frac{\partial N}{\partial r} \right) + \frac{\partial^2 N}{\partial z^2} \right\} - V_c \text{sign}(z) \frac{\partial N}{\partial z} - v \sigma_{\text{ism}} \delta(z) N . \quad (\text{A2})$$

The Galaxy is modelled as a flat disk that rotates around the vertical direction Oz . As boundaries in the radial direction r play little role in our analysis, the disk is assumed to be the infinite plane $\{O, x, y\}$. It is furthermore sandwiched by two confinement layers that extend to $z = \pm L$. The aim of this section is to derive the contribution of a source S located at $\{x = 0, y = 0, z = s\}$ and exploding at time $t = 0$ to the subsequent cosmic-ray density anywhere else in the Galaxy at location $P \{x, y, z\}$. The initial density reduces to the Dirac distribution

$$N \{S, 0 \rightarrow P, 0\} \equiv \delta(x) \delta(y) \delta(z - s) , \quad (\text{A3})$$

and we would like to compute it at any time $t > 0$. Should there be no vertical boundaries, no galactic wind and no spallations, the solution would be given by mere diffusion in infinite space

$$N \{S, 0 \rightarrow P, t \geq 0\} = \left\{ \frac{1}{4 \pi K t} \right\}^{3/2} \exp \left\{ -\frac{r^2}{4 K t} \right\} \exp \left\{ -\frac{(z - s)^2}{4 K t} \right\} , \quad (\text{A4})$$

with $r^2 = x^2 + y^2$. The previous relation together with the fact that the diffusion processes in the z direction and in the radial direction are independent from each other suggest that the solution to equation (A2) should be factorized into

$$N \{S, 0 \rightarrow P, t \geq 0\} = \frac{1}{4 \pi K t} \exp \left\{ -\frac{r^2}{4 K t} \right\} n \{s, 0 \rightarrow z, t \geq 0\} . \quad (\text{A5})$$

A.2. Resolution

Equation (A2) has now simplified into

$$\frac{\partial n}{\partial t} = K \frac{\partial^2 n}{\partial z^2} - V_c \text{sign}(z) \frac{\partial n}{\partial z} - v\sigma \Sigma_{\text{ism}} \delta(z) n \quad , \quad (\text{A6})$$

and the trick is to factorize once again the time t and the vertical z behaviors so that $n \equiv f(z)g(t)$. The resulting solution may appear contrived and exceptional. Actually an infinite set of such functions obtains that turns out to be a natural basis for the generic solutions to equation (A6). The time behavior amounts to the exponential decrease $g(t) = \exp(-\alpha t)$ where the positive constant α also appears in the vertical behavior

$$K \frac{\partial^2 f}{\partial z^2} - V_c \text{sign}(z) \frac{\partial f}{\partial z} - v\sigma \Sigma_{\text{ism}} \delta(z) f + \alpha f = 0 \quad . \quad (\text{A7})$$

We would like to derive the solution $f(z)$ with the condition that it must vanish on the boundaries at $z = \pm L$. In the upper confinement layer where $0 < z \leq L$, the vertical equation simplifies even further into

$$K f'' - V_c f' + \alpha f = 0 \quad , \quad (\text{A8})$$

and has two solutions depending on the value of α .

- For $V_c^2 - 4K\alpha > 0$, we readily obtain

$$f(z) \propto e^{z/r_w} \sinh \{ \beta (L - z) \} \quad , \quad (\text{A9})$$

where $r_w = 2K/V_c$ and $\beta = \{V_c^2 - 4K\alpha\}^{1/2}/2K$. That kind of exponential solution does not fulfil the disk crossing condition or cannot lead to continuous odd functions of z – see below. We will therefore shortly disregard it.

- More interesting is the case for which $V_c^2 - 4K\alpha < 0$. The solution reads

$$f(z) \propto e^{z/r_w} \sin \{ k (L - z) \} \quad , \quad (\text{A10})$$

where the wavevector $k = \{4K\alpha - V_c^2\}^{1/2}/2K$.

The solution $f(z)$ is a continuous function. Integrating the differential equation (A7) across the disk leads to a relation between f and its derivatives

$$K \{ f'(0_+) - f'(0_-) \} - 2V_c f(0) - v\sigma \Sigma_{\text{ism}} f(0) = 0 \quad . \quad (\text{A11})$$

Notice that odd functions of z readily satisfy this condition insofar as they vanish at $z = 0$ and have even derivatives so that $f'(0_+)$ and $f'(0_-)$ are equal. On the contrary, the disk crossing

condition (A11) sets severe constraints on even functions. In particular, the exponential solution (A9) turns out to be forbidden. On the contrary, the solution (A10) fulfills the disk crossing condition provided that the wavevector k satisfies the equation

$$\tan(kL) \cdot \left\{ \frac{L}{r_s} + \frac{L}{r_w} \right\} = -kL \quad , \quad (\text{A12})$$

where we have introduced the typical length $r_s = K/h\Gamma$. An infinite set of wavevectors k_n obtains so that the series of functions

$$f_{+n}(z) = e^{|z|/r_w} \sin \{k_n (L - |z|)\} \quad , \quad (\text{A13})$$

turns out to be the solution looked for in the case of an even parity with respect to z . In the regime where the galactic wind and the spallations are negligible with respect to diffusion, both r_s and r_w are infinite and the wavevectors are given by $k_n L = (n - 1/2) \pi$. In the opposite regime, we get $k_n L = n\pi$. Because the exponential vertical behavior $\exp(|z|/r_w)$ is the same for all the modes n , it is convenient to define the basis of eigenvectors $\varphi_n(z) = \sin \{k_n (L - |z|)\}$ so that any even solution $f_+(z)$ to our problem may be expanded as

$$f_+(z) = e^{|z|/r_w} \sum_{n=1}^{+\infty} a_n \varphi_n(z) \quad . \quad (\text{A14})$$

The coefficients a_n are the coordinates of $f(z)$ in the basis of the vectors φ_n . For odd functions, we require the solution to be continuous at the disk and therefore to vanish for $z = 0$. This eliminates once again the exponential possibility (A9) to the advantage of the other option (A10). The series of functions

$$f_{-n}(z) = e^{|z|/r_w} \{ \varphi'_n(z) \equiv \sin(k'_n [L - z]) \} \quad (\text{A15})$$

obtains with the requirement that $k'_n L = n\pi$. Any initial vertical distribution $n(z, 0)$ may therefore be expanded in terms of the even φ_n and odd φ'_n modes

$$n(z, 0) = e^{|z|/r_w} \sum_{n=1}^{+\infty} \{ a_n \varphi_n(z) + b_n \varphi'_n(z) \} \quad . \quad (\text{A16})$$

Each of these modes decays exponentially in time and the initial distribution subsequently evolves into

$$n(z, t \geq 0) = e^{|z|/r_w} \sum_{n=1}^{+\infty} \left\{ a_n e^{-\alpha_n t} \varphi_n(z) + b_n e^{-\alpha'_n t} \varphi'_n(z) \right\} \quad , \quad (\text{A17})$$

where $\alpha_n = K \{k_n^2 + (V_c/2K)^2\}$ while $\alpha'_n = K \{k_n'^2 + (V_c/2K)^2\}$. We can push forward the analogy between functions and vectors by defining the hermitian product between $a(z)$ and $b(z)$ by

$$\langle b|a \rangle = \int_{-L}^{+L} b^*(z) a(z) dz , \quad (\text{A18})$$

where b^* denotes the complex conjugate of b . As solutions of a Schrödinger-like equation, the vectors φ_n and φ'_n form an orthogonal set,

$$\langle \varphi_p|\varphi_n \rangle = C_n \delta_{pn} = L \left\{ 1 + \left(\frac{L}{r_s} + \frac{L}{r_w} \right) \sin_c^2(k_n L) \right\} \delta_{pn} , \quad (\text{A19})$$

whereas

$$\langle \varphi'_p|\varphi_n \rangle = 0 \quad \text{and} \quad \langle \varphi'_p|\varphi'_n \rangle = C'_n \delta_{pn} = L \delta_{pn} . \quad (\text{A20})$$

In the case of the initial distribution $n \{s, 0 \rightarrow z, 0\} = \delta(z - s)$, the coefficients a_n and b_n are found by mere projection on the basis vectors

$$a_n = \frac{e^{-|s|/r_w}}{C_n} \sin \{k_n (L - |s|)\} \quad \text{while} \quad b_n = \frac{e^{-|s|/r_w}}{C'_n} \sin \{k'_n (L - s)\} . \quad (\text{A21})$$

As a result, the Green function that accounts for the propagation of a cosmic-ray particle from the source S at $t = 0$ to the observer P at time t may be expressed as

$$\begin{aligned} N \{S, 0 \rightarrow P, t \geq 0\} &= \frac{1}{4\pi K t} \exp \left\{ -\frac{r^2}{4K t} \right\} e^{(|z|-|s|)/r_w} \times \\ &\times \sum_{n=1}^{+\infty} \left\{ \frac{e^{-\alpha_n t}}{C_n} \varphi_n(s) \varphi_n(z) + \frac{e^{-\alpha'_n t}}{C'_n} \varphi'_n(s) \varphi'_n(z) \right\} . \end{aligned} \quad (\text{A22})$$

This solution takes into account the presence of vertical boundaries at $z = \pm L$ as well as the existence of a galactic wind and of spallations in the disk. Should we focus on supernovae sources S located in the galactic ridge where $s = 0$, that expression would simplify into a series of even contributions only

$$N \{S, 0 \rightarrow P, t\} = \frac{e^{-r^2/4Kt}}{4\pi K t} e^{|z|/r_w} \sum_{n=1}^{+\infty} \frac{e^{-\alpha_n t}}{C_n} \sin \{k_n L\} \sin \{k_n (L - |z|)\} . \quad (\text{A23})$$

A.3. The method of images

In the absence of galactic wind and of disk spallations – in the regime where r_s and r_w are infinite – a completely different approach is provided by the elegant method of the

images inspired from electrostatics. In infinite space, the solution to our diffusion problem is straightforward and is given by relation (A4) in the case of an initial Dirac distribution at the source S . We furthermore would like to impose the boundary condition according to which the cosmic-ray density N vanishes on the plane $z = +L$ at any time. To do so, we can introduce the virtual source S' that is the image of the real source S with respect to the boundary $z = +L$ acting like a mirror. The cosmic-ray densities which S and its image S' generate are equal up to a relative minus sign that allows both contributions to cancel out exactly on the boundary. The distribution of sources within the Galaxy is not perturbed by the presence of their virtual images that are located outside the domain of interest. In order to impose that the density also vanishes at $z = -L$, we can consider the image S'' of S with respect to that lower boundary and assume that it also generates the opposite density with respect to S . Because two mirrors are now present at $z = +L$ and $z = -L$, an infinite series of multiple images $\{S_n\}$ arises. They are aligned with the real source $S_0 \equiv S$ in the vertical direction and the position of S_n is given by

$$s_n = 2Ln + (-1)^n s . \quad (\text{A24})$$

The virtual source S_n results from $|n|$ reflections throughout the mirrors and its production is affected by a sign $(-1)^n$ with respect to the real source S . We readily infer that in the presence of boundaries, the solution (A4) is modified into

$$N \{S, 0 \rightarrow P, t\} = \frac{e^{-r^2/4Kt}}{4\pi Kt} \times \left\{ n \{s, 0 \rightarrow z, t\} = \sum_{n=-\infty}^{+\infty} \frac{(-1)^n}{\sqrt{4\pi Kt}} e^{-(z-s_n)^2/4Kt} \right\} . \quad (\text{A25})$$

The diffusion processes along the vertical axis and in the radial direction have decoupled. The diffusion from the single source S within a slab – on the boundaries of which the cosmic-ray density vanishes – amounts simply to the diffusion in infinite space from the series of sources S_n . Along the vertical direction, the initial distribution is

$$n \{s, 0 \rightarrow z, 0\} = \sum_{n=-\infty}^{+\infty} (-1)^n \delta(z - s_n) . \quad (\text{A26})$$

Because that distribution is periodic, its Fourier transform which we define by

$$N(k) = \int_{-\infty}^{+\infty} n \{s, 0 \rightarrow z, 0\} e^{-ikz} dz , \quad (\text{A27})$$

is composed of a discrete series of modes k . It may actually be expressed as

$$N(k) = \sum_{n=-\infty}^{+\infty} (-1)^n e^{-iks_n} \equiv \left\{ e^{-iks} - e^{2kL} e^{iks} \right\} \left\{ \mathcal{S} = \sum_{n=-\infty}^{+\infty} e^{-4inkL} \right\} . \quad (\text{A28})$$

After some straightforward algebra, the sum \mathcal{S} is transformed into

$$\mathcal{S} = \frac{\pi}{2L} \sum_{n=-\infty}^{+\infty} \delta \left(k - n \frac{\pi}{2L} \right) . \quad (\text{A29})$$

We conclude that the initial vertical distribution $n \{s, 0 \rightarrow z, 0\}$ contains a series of modes with discrete wavevectors $k = n\pi/2L$. Odd values of $n = 2p - 1$ are associated to modes for which $k_p L = (p - 1/2) \pi$ and contribute a factor

$$N(k_p) = \frac{\pi}{L} \cos k_p s , \quad (\text{A30})$$

whereas even values of $n = 2p$ lead to wavevectors k'_p such that $k'_p L = p\pi$ and to

$$N(k'_p) = -i \frac{\pi}{L} \sin k'_p s . \quad (\text{A31})$$

The initial cosmic-ray distribution in the vertical direction $n \{s, 0 \rightarrow z, 0\}$ may be expressed as a Fourier series on the various odd and even modes p which we have just scrutinized

$$n \{s, 0 \rightarrow z, 0\} = \sum_{p=1}^{+\infty} \frac{1}{L} \cos(k_p s) \cos(k_p z) + \frac{1}{L} \sin(k'_p s) \sin(k'_p z) . \quad (\text{A32})$$

Because each Fourier mode k exponentially decays in time like $\exp(-Kk^2 t)$ as a result of diffusion, the initial distribution subsequently evolves into

$$n \{s, 0 \rightarrow z, t\} = \sum_{p=1}^{+\infty} \frac{e^{-Kk_p^2 t}}{L} \cos(k_p s) \cos(k_p z) + \frac{e^{-Kk'^2_p t}}{L} \sin(k'_p s) \sin(k'_p z) . \quad (\text{A33})$$

The careful reader will have certainly noticed that we have just recovered expression (A22)

$$n \{s, 0 \rightarrow z, t\} = \sum_{p=1}^{+\infty} \frac{e^{-\alpha_p t}}{C_p} \varphi_p(s) \varphi_p(z) + \frac{e^{-\alpha'_p t}}{C'_p} \varphi'_p(s) \varphi'_p(z) , \quad (\text{A34})$$

from which the galactic wind and the spallations are absent. In that regime, the wavevectors $k_p = (p - 1/2) \pi/L$ and $k'_p = p\pi/L$ are actually the same in both analysis. The normalization constants are $C_p = C'_p = L$ whereas $\alpha_p = Kk_p^2$ and $\alpha'_p = Kk'^2_p$ since $V_c = 0$. Finally, the basis vectors $\varphi_p(z)$ and $\varphi'_p(z)$ are respectively given by

$$\varphi_p(z) \equiv \sin \{k_p (L - |z|)\} = (-1)^{p+1} \cos k_p z , \quad (\text{A35})$$

whereas

$$\varphi'_p(z) \equiv \sin \{k'_p (L - z)\} = (-1)^{p+1} \sin k'_p z . \quad (\text{A36})$$

The general resolution that has been discussed in section (A.2) leads to the same result as the method of images presented here.

B. Path-length distribution for a non homogeneous spallative disk

We now solve Eq. (6) in the case under study, for the steady-state case

$$0 = K \left\{ \frac{1}{r} \frac{\partial}{\partial r} (r \mathcal{N}(r, z, x)) + \frac{\partial^2 \mathcal{N}(r, z, x)}{\partial z^2} \right\} + q(r) \delta(z) \delta(x) - \frac{\partial \mathcal{N}(r, z, x)}{\partial x} v \sigma \Sigma_{\text{ism}}^0 f(r) \delta(z)$$

with $f(r) \equiv \Sigma_{\text{ism}}(r)/\Sigma_{\text{ism}}^0$ and $\Sigma_{\text{ism}}^0 = 6.2 \cdot 10^{20} \text{ cm}^{-2}$ (Ferrière (1998)). We perform Fourier-Bessel transforms using the J_0 functions,

$$\mathcal{N}(r, z, x) = \sum_{i=0}^{\infty} \mathcal{N}_i(z, x) J_0 \left(\zeta_i \frac{r}{R} \right) \quad \text{and} \quad f(r) \mathcal{N}(r, z=0, x) = \sum_{i=0}^{\infty} f_i(x) J_0 \left(\zeta_i \frac{r}{R} \right)$$

with

$$\begin{aligned} \mathcal{N}_i(z, x) &= \frac{2}{J_1^2(\zeta_i)} \int_0^1 \rho J_0(\zeta_i \rho) \mathcal{N}(\rho R, z, x) d\rho \\ f_i(x) &= \frac{2}{J_1^2(\zeta_i)} \int_0^1 \rho J_0(\zeta_i \rho) f(\rho R) \mathcal{N}(\rho R, z=0, x) = \sum_{j=0}^{\infty} \alpha_{ij} \mathcal{N}_j(0, x) \end{aligned}$$

where we have introduced the matrix

$$\alpha_{ij} = \frac{2}{J_1^2(\zeta_i)} \int_0^1 \rho J_0(\zeta_i \rho) J_0(\zeta_j \rho) f(\rho R) d\rho$$

These expressions are reminiscent of those of Wallace (1981) that was dedicated to a perturbative resolution of the diffusion equation in the presence of an arbitrary matter distribution (he do not determine the path-length distribution, though). The generalized diffusion equation reads

$$0 = K \left\{ \frac{\zeta_i^2}{R^2} \mathcal{N}_i(z, x) + \frac{\partial^2 \mathcal{N}_i(z, x)}{\partial z^2} \right\} + q_i \delta(z) \delta(x) - \frac{\partial f_i(x)}{\partial x} v \sigma \Sigma_{\text{ism}}^0 \delta(z) \quad (\text{B1})$$

The solution for $z \neq 0$ satisfying $f(z = \pm L, x) = 0$ is

$$\mathcal{N}_i(z, x) = \mathcal{N}_i(0, x) \frac{\sinh(\zeta_i(L - |z|)/R)}{\sinh(\zeta_i L/R)}$$

This expression is inserted back in the diffusion equation, taking care of the singularity of $|z|$ in 0 by using

$$\frac{\partial^2 \mathcal{N}_i(z, x)}{\partial z^2} = \frac{\zeta_i^2}{R^2} \mathcal{N}_i(z, x) + \mathcal{N}_i(0, x) \frac{2\zeta_i}{R} v \sigma \Sigma_{\text{ism}}^0 \delta(z) \coth \left(\frac{\zeta_i L}{R} \right)$$

which yields

$$0 = K \mathcal{N}_i(0, x) \frac{2\zeta_i}{R} \coth \left(\frac{\zeta_i L}{R} \right) + q_i \delta(x) - v \sigma \Sigma_{\text{ism}}^0 \sum_{j=0}^{\infty} \alpha_{ij} \frac{\partial \mathcal{N}_j(0, x)}{\partial x}$$

or

$$0 = \mathcal{N}_i(0, x) + \frac{q_i}{K} \frac{R}{2\zeta_i} \tanh\left(\frac{\zeta_i L}{R}\right) \delta(x) - \frac{v\sigma\Sigma_{\text{ism}}^0 R}{2\zeta_i K} \tanh\left(\frac{\zeta_i L}{R}\right) \sum_{j=0}^{\infty} \alpha_{ij} \frac{\partial \mathcal{N}_j(0, x)}{\partial x} \quad (\text{B2})$$

The solutions of this linear set of coupled first order differential equations are

$$\mathcal{N}_i(0, x) = \sum_{j=0}^{\infty} a_{ij} e^{-x/x_j} \Theta(x) \quad (\text{B3})$$

where the x_j are the eigenvalues of the matrix

$$A_{ij} = \frac{v\sigma\Sigma_{\text{ism}}^0 R}{2K\zeta_i} \tanh\left(\frac{\zeta_i L}{R}\right) \alpha_{ij}$$

Indeed, inserting expression (B3) in (B1), and using

$$\frac{\partial \mathcal{N}_j(0, x)}{\partial x} = - \sum_{k=0}^{\infty} \frac{a_{jk}}{x_k} e^{-x/x_k} \Theta(x) + \delta(x) \sum_{k=0}^{\infty} a_{jk}$$

we find an equation that can be separated in a regular part (factor of $\Theta(x)$) and a singular part (factor of $\delta(x)$). The former reads

$$\sum_{j=0}^{\infty} a_{ij} e^{-x/x_j} - \frac{v\sigma\Sigma_{\text{ism}}^0 R}{2\zeta_i K} \tanh\left(\frac{\zeta_i L}{R}\right) \sum_{k=0}^{\infty} \alpha_{ik} \sum_{j=0}^{\infty} \frac{a_{kj}}{x_j} e^{-x/x_j} = 0$$

In order for each coefficient of e^{-x/x_j} to be zero, one must have

$$a_{ij} - \frac{v\sigma\Sigma_{\text{ism}}^0 R}{2\zeta_i K x_j} \tanh\left(\frac{\zeta_i L}{R}\right) \sum_{k=0}^{\infty} \alpha_{ik} a_{kj} = 0 \quad (\text{B4})$$

so that

$$\det \left[x_j \delta_{ik} - \frac{v\sigma\Sigma_{\text{ism}}^0 R}{2\zeta_i K} \tanh\left(\frac{\zeta_i L}{R}\right) \alpha_{ik} \right] = 0 \quad (\text{B5})$$

This shows that the x_i are eigenvalues of A_{ij} . This equation alone is then not enough to compute the a_{ij} . An extra relation is provided by the singular part

$$- \frac{v\sigma\Sigma_{\text{ism}}^0 R}{2\zeta_i K} \tanh\left(\frac{\zeta_i L}{R}\right) \sum_{j=0}^{\infty} \alpha_{ij} \sum_{k=0}^{\infty} a_{jk} = - \frac{q_i}{K} \frac{R}{2\zeta_i} \tanh\left(\frac{\zeta_i L}{R}\right)$$

which gives

$$\sum_{k=0}^{\infty} \sum_{j=0}^{\infty} \alpha_{ij} a_{jk} = \frac{q_i}{v\sigma\Sigma_{\text{ism}}^0} \quad (\text{B6})$$

The coefficients a_{ij} are completely set by Eqs (B5) and (B6).

When the galactic wind is taken into account, a more tedious derivation shows that Eq. (B2) is replaced by

$$0 = \mathcal{N}_i(0, x) + \frac{q_i}{2K} \left[\frac{1}{r_w} + S_i \coth \left(\frac{\zeta_i L}{R} \right) \right]^{-1} \delta(x) - \frac{v\sigma\Sigma_{\text{ism}}^0}{2K} \left[\frac{1}{r_w} + S_i \coth \left(\frac{\zeta_i L}{R} \right) \right]^{-1} \sum_{j=0}^{\infty} \alpha_{ij} \frac{\partial \mathcal{N}_j(0, x)}{\partial x} \quad (\text{B7})$$

so that the same results apply, provided that one makes the substitution

$$\frac{R}{2\zeta_i} \tanh \left(\frac{\zeta_i L}{R} \right) \rightarrow \left(\frac{1}{r_w} + S_i \coth \left(\frac{S_i L}{2} \right) \right)^{-1} \quad \text{and} \quad S_i = 2 \left(\frac{1}{r_w^2} + \frac{\zeta_i^2}{R^2} \right)^{1/2}$$

C. Linear galactic wind in the steady-state cylindrical disk-halo model

Resolution of the diffusion equation for a stable primary We write $V_c(z) = V_0 z$, and the steady-state diffusion equation reads (see also Bloemen et al. (1993))

$$0 = \frac{K}{r} \frac{\partial}{\partial r} \left\{ r \frac{\partial N}{\partial r} \right\} - \frac{\partial N}{\partial z} \left\{ -K \frac{\partial N}{\partial z} + V_0 z N \right\} - \sigma \Sigma v \delta(z) N + 2hq \delta(z)$$

Developing over Bessel functions,

$$-\frac{2hq_i}{K} \delta(z) = -\frac{\zeta_i^2}{R^2} N_i + \frac{\partial^2 N_i}{\partial z^2} - \frac{V_0 z}{K} \frac{\partial N_i}{\partial z} - \frac{V_0}{K} N_i - \frac{\sigma \Sigma v}{K} \delta(z) N_i$$

It is convenient to rewrite this equation in a hermitic differential form, to ensure that the solutions form an orthogonal set of functions (see e.g. Morse & Feshbach). We introduce $\beta = V_0/4K$ and $y = kz$ with $k = \sqrt{V_0/2K}$, which yields, in the halo

$$n_i'' - n_i (a_i + y^2) = 0$$

where

$$a_i \equiv \frac{2K}{V_0} \frac{\zeta_i^2}{R^2} + 2$$

The solutions are of the form, taking into account the condition $n(z = \pm L) = 0$,

$$n = B_i e^{-k^2 z^2/2} \left\{ \phi \left(\frac{1+a_i}{4}, \frac{1}{2}; k^2 z^2 \right) - \frac{z}{L} \frac{\phi \left(\frac{1+a_i}{4}, \frac{1}{2}; k^2 L^2 \right)}{\phi \left(\frac{3+a_i}{4}, \frac{3}{2}; k^2 L^2 \right)} \phi \left(\frac{3+a_i}{4}, \frac{3}{2}; k^2 z^2 \right) \right\}$$

where ϕ is the confluent hypergeometric function, also noted ${}_1F_1$. The constant B_i is found by integrating the diffusion equation through the disk, so that

$$2 \left. \frac{dn_i}{dz} \right|_{z=0} = \frac{\sigma \Sigma v}{K} n_i(0) - \frac{2hq_i}{K}$$

This gives $B_i = 2hq_i/A_i$ with

$$A_i = \frac{2K}{L} \frac{\phi\left(\frac{1+a_i}{4}, \frac{1}{2}; k^2 L^2\right)}{\phi\left(\frac{3+a_i}{4}, \frac{3}{2}; k^2 L^2\right)} + v\sigma \Sigma_{\text{ism}}^0 \quad (\text{C1})$$

The final solution is thus obtained as

$$N(r, z) = \sum_i \frac{q_i}{A_i} J_0\left(\zeta_i \frac{r}{R}\right) \left\{ \phi\left(\frac{1+a_i}{4}, \frac{1}{2}; k^2 z^2\right) - \frac{z}{L} \frac{\phi\left(\frac{1+a_i}{4}, \frac{1}{2}; k^2 L^2\right)}{\phi\left(\frac{3+a_i}{4}, \frac{3}{2}; k^2 L^2\right)} \phi\left(\frac{3+a_i}{4}, \frac{3}{2}; k^2 z^2\right) \right\} \quad (\text{C2})$$

The density in the disk is thus given by

$$N(r, z=0) = \sum_i \frac{2hq_i}{A_i} J_0\left(\zeta_i \frac{r}{R}\right) \quad (\text{C3})$$

It can be shown that this expression reduces to the usual expressions in the case of a vanishing wind.

The path-length distribution The dependence in σ is very simple and the path-length distribution is obtained by inverse Laplace transform as

$$N(r, z, x) = \sum_i 2hq_i J_0\left(\zeta_i \frac{r}{R}\right) \exp\left(-\frac{x}{x_i}\right) \Theta(x)$$

with

$$x_i = \frac{mv\Sigma L}{2K} \frac{\phi\left(\frac{5}{4} + \frac{K}{2V_0} \frac{\zeta_i^2}{R^2}, \frac{3}{2}; \frac{V_0 L^2}{2K}\right)}{\phi\left(\frac{3}{4} + \frac{K}{2V_0} \frac{\zeta_i^2}{R^2}, \frac{1}{2}; \frac{V_0 L^2}{2K}\right)}$$

REFERENCES

- Aharonian, F. A., Atoyan, A. M., Völk, H. J., 1995, *A&A*, 294, L41
- Benítez, N., Maíz-Apellániz, J. and Canelles, M., 2002, *Physical Review Letters*, 88, 81101
- Bloemen, J. B. G. M., Dogiel, V. A., Dorman, V. L. and Ptuskin, V. S., 1993, *A&A*, 267, 372
- Cowsik, R. and Lee, M. A., 1979, *ApJ*, 228, 297
- Donato, F., Maurin, D., Taillet, R., 2002, *A&A*, 381, 539
- Dorman, L. I., Ghosh, A. and Ptuskin, V. S., 1985, *Ap&SS*, 109, 87
- Erlykin, A. D. and Wolfendale, A. W., 2001a, *J.Physics G: Nucl. Part. Phys.*, 27, 941
- Erlykin, A. D. and Wolfendale, A. W., 2001b, *J.Physics G: Nucl. Part. Phys.*, 27, 959
- Ferrière, K., 1998, *ApJ*, 497, 759
- Fields, B. D., Ellis, J., 1999, *New Astronomy*, 4, 419
- Forman, M. A. and Schaeffer, O. A., 1979, *Reviews of Geophysics and Space Physics*, 17, 552
- Freedman, I., Giler, M., Kearsy, S. and Osborne, J. L., 1980, *A&A*, 82, 110
- Higdon, J. C. and Lingelfelter, R. E., 2003, *ApJ*, 582, 330
- Jones, F. C., 1979, *ApJ*, 229, 747
- Johnson, 1994, *Astroparticle Physics*, 2, 257
- Knie, K., Korschinek, G., Faestermann, T., Wallner, C., Scholten, J., Hillebrandt, W., 1999, *Physical Review Letters*, 83, 18
- Lerche, I. and Schlickeiser, R., 1982, *A&A*, 116, 10
- Lezniak, J. A., 1979, *Ap&SS*, 63, 279
- Lezniak, J. A., and Webber, W. R., 1979, *Ap&SS*, 63, 35
- Margolis, S. H., 1986, *ApJ*, 300, 20
- Maurin, D.; Donato D., Taillet, R. and Salati, P., 2001, *ApJ*, 555, 585

- Owens, A. J., 1976, *Ap&SS*, 44, 35
- Ramadurai, 1993, *Bull. Astr. Soc. India*, 21, 391
- Shaviv, N. J., 2002, *Physical Review Letters*, 89, 51102
- Stephens, S. A. and Streitmatter, R. E., 1998, *ApJ*, 505, 266
- Taillet, R., and Maurin, D., 2003, *A&A*, 402, 971
- Wallace, J. M., 1981, *ApJ*, 245, 753
- Webber, W. R., et al., 1998, *ApJ*, 508, 940

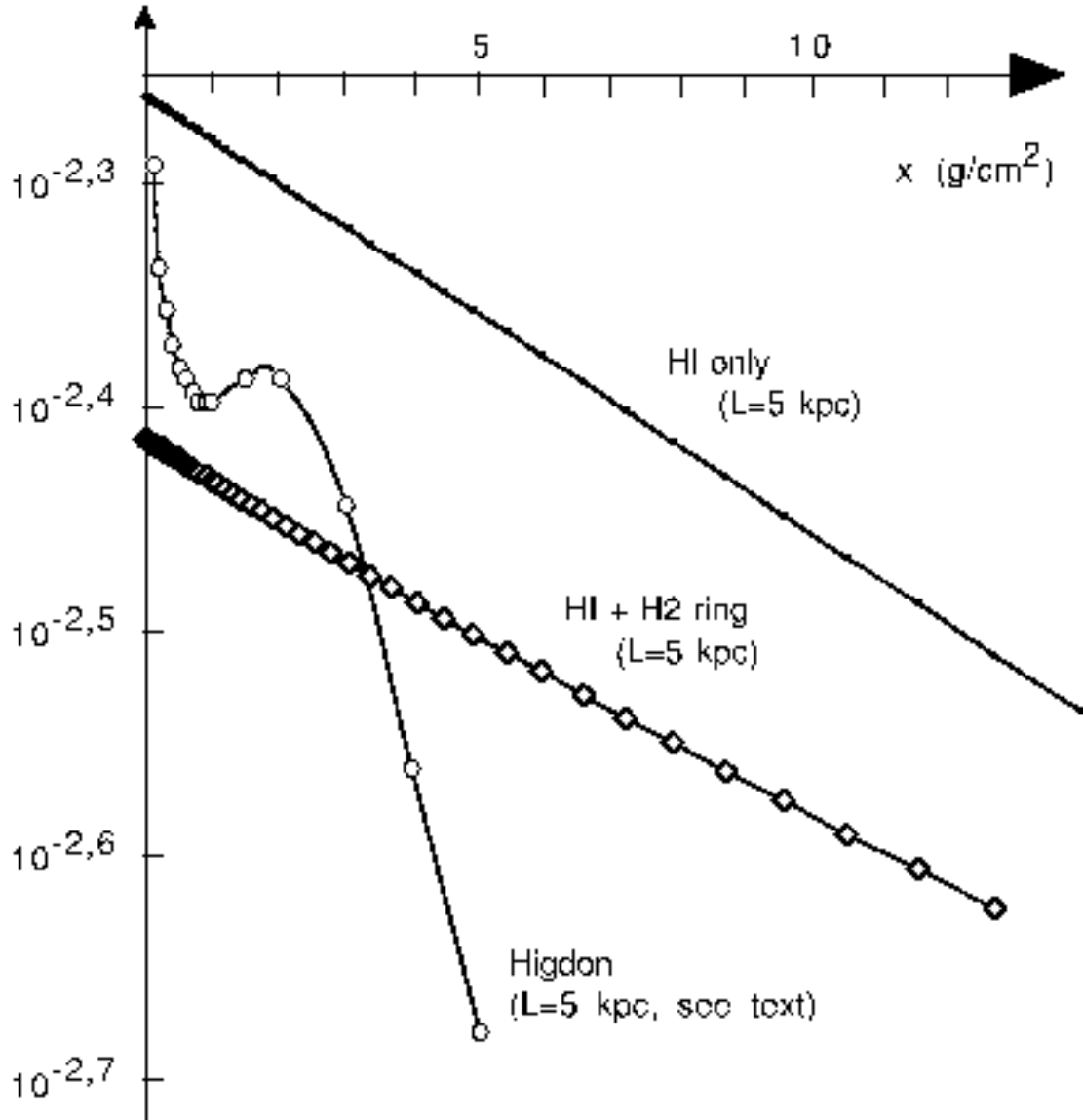


Fig. 1.— Path-length distribution (x in g cm^{-2}) for a homogeneous disk distribution ($L = 5$ kpc, black dots) and with an additional H_2 ring, radially distributed according to Hidgon (squares). The feature at high grammage, visible in the Hidgon points (circles) is not reproduced by the analytical result.

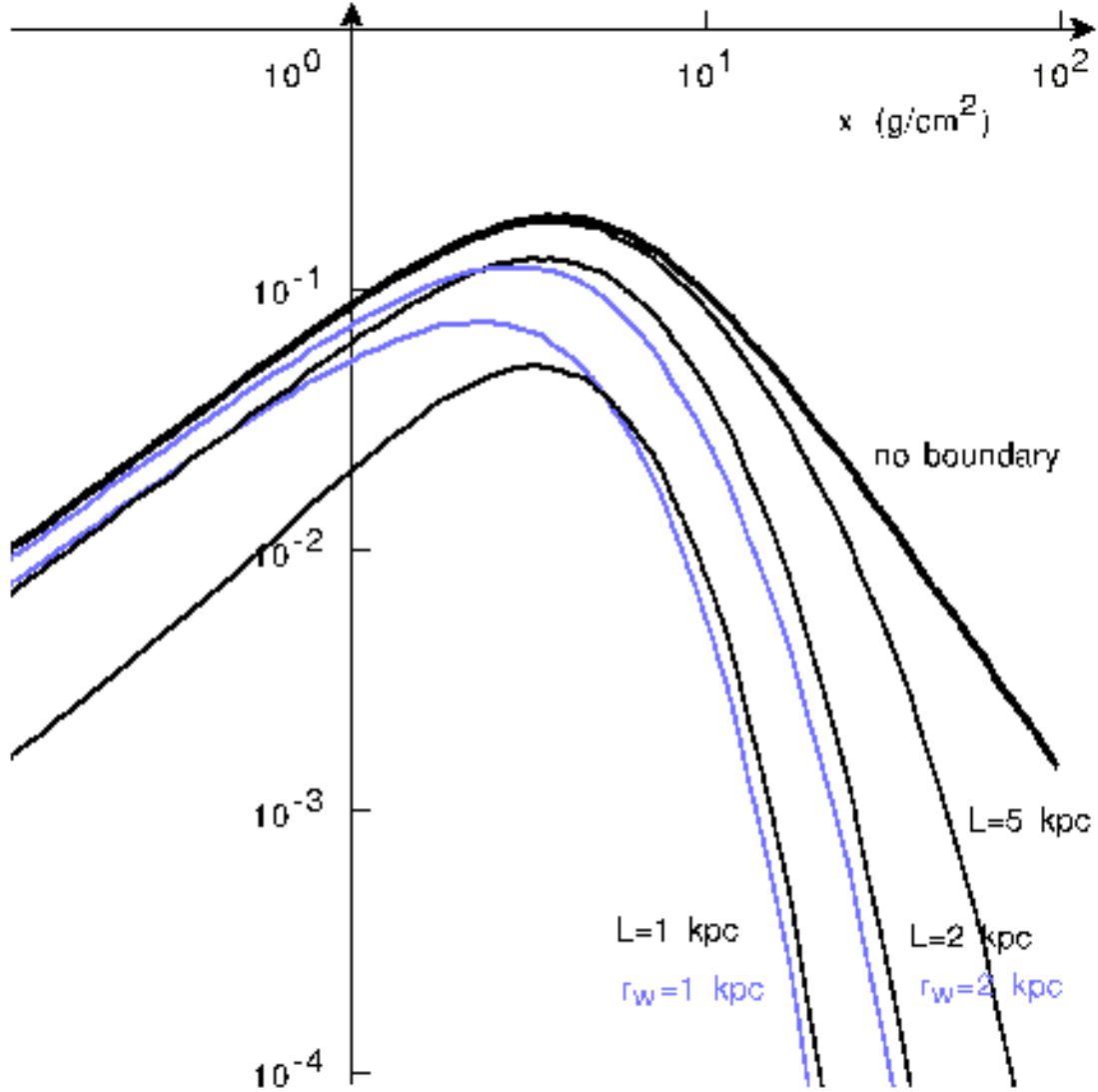


Fig. 2.— Path-length distributions (x in g cm^{-2}) are shown for a point source located at a distance $r = 1$ kpc, and for different propagation conditions. The thick line corresponds to free diffusion (no boundary, no wind). The thin black lines show the influence of escape for $L = 1, 2$ and 5 kpc. The higher grammages, corresponding to longer paths, are more suppressed by escape, which shifts the maximum of the path-length distribution towards low grammages. The effect of the convective wind, displayed as light lines for $r_w = 1$ and 2 kpc, is similar though quantitatively different for low grammages (see text for a discussion). The overall normalisation is decreased when escape and/or wind are considered, which reflects the corresponding decrease of flux.

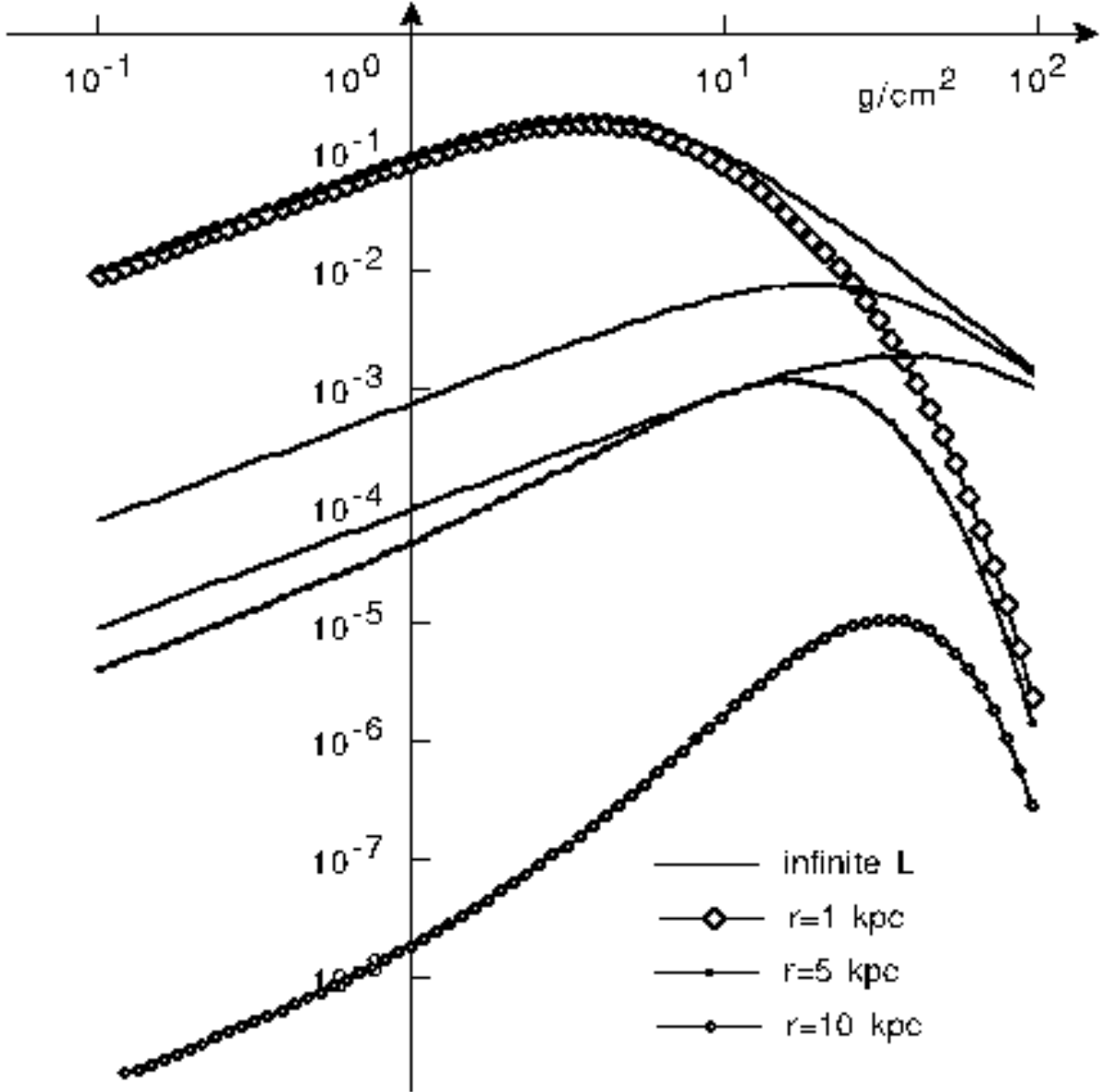


Fig. 3.— The path-length distribution (x in g cm^{-2}) is shown for a point source and for different r . The two situations $L = 5$ kpc and L infinite are shown for comparison. The short grammages are depleted for remote sources, as the probability to travel a long distance without crossing the disc is small. This effect is all more pronounced that L is small. The normalisation also decreases with L , which reflects the corresponding decrease of flux.

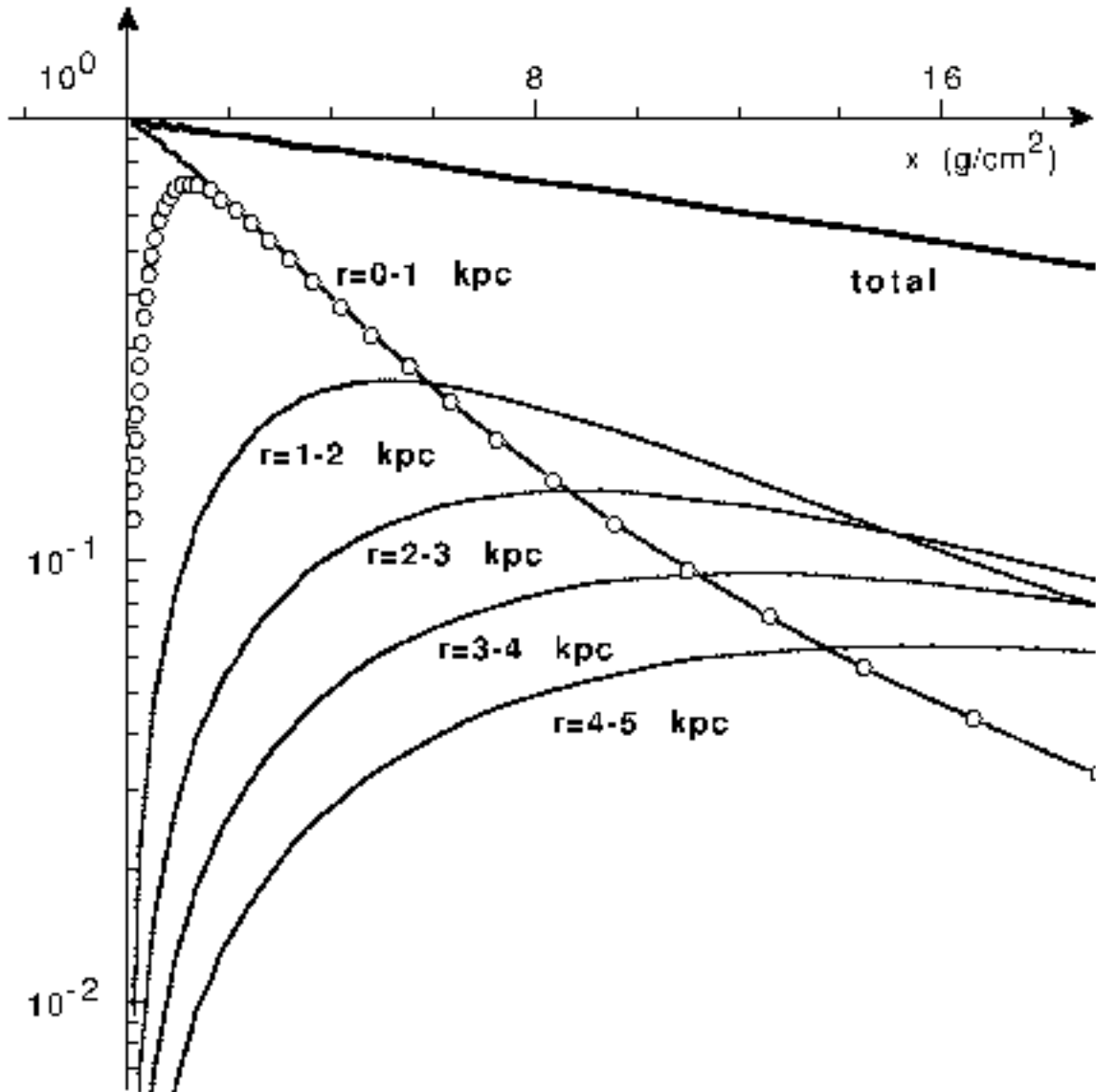


Fig. 4.— The contributions to the path-length distribution (thick line) from continuous sources distributed in several rings (thin lines) are displayed for $L = 5$ kpc. The path-length distribution from a set of 100 point sources drawn randomly in the central ring (inner 1 kpc) is also shown (black dots). The effect of discreteness is most visible for low grammages. For the other rings, the difference between the continuous distribution and 100 discrete sources is of the order of a percent.

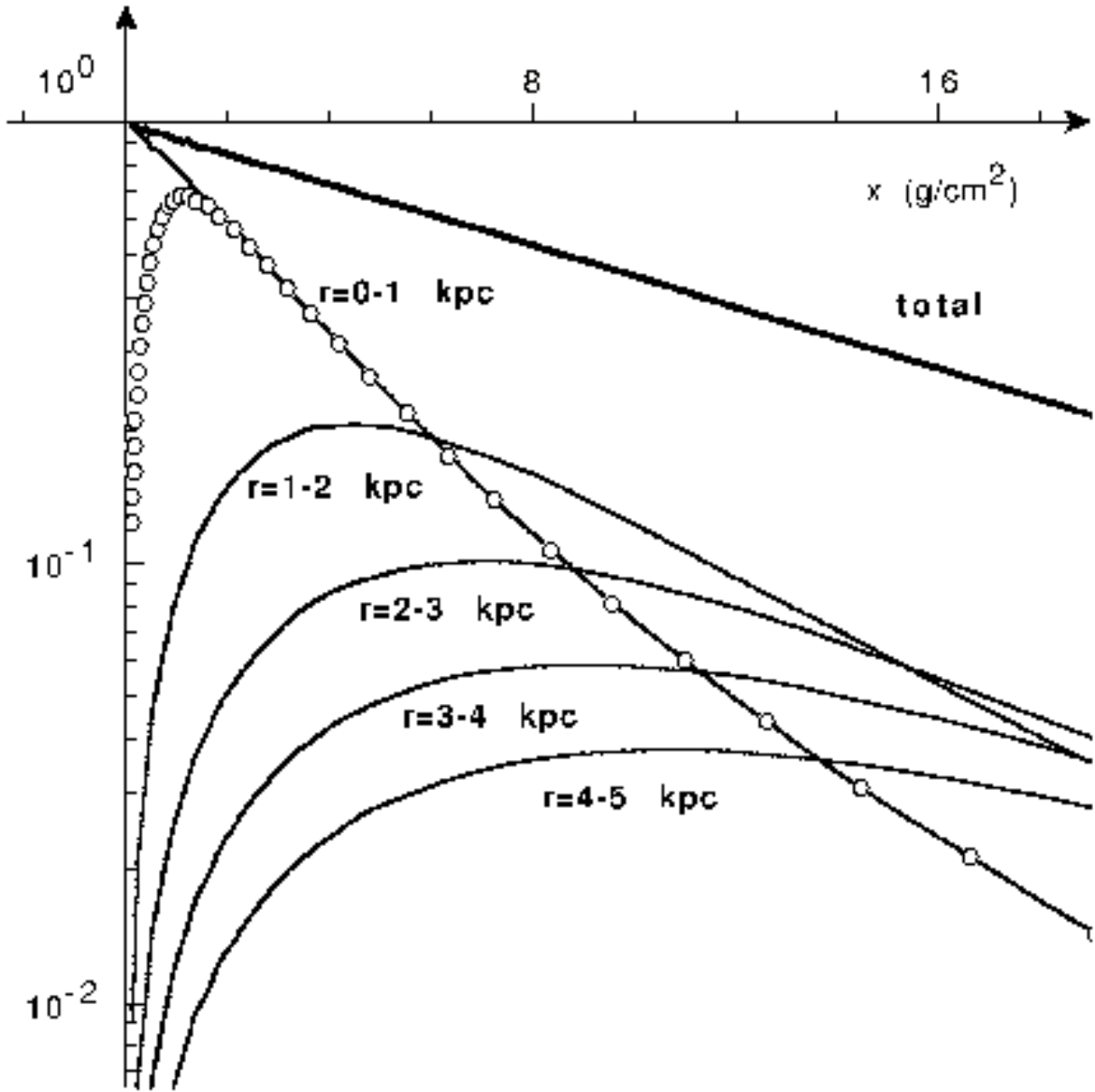


Fig. 5.— Same as the previous figure, for $r_w = 5 \text{ kpc}$ and L infinite.

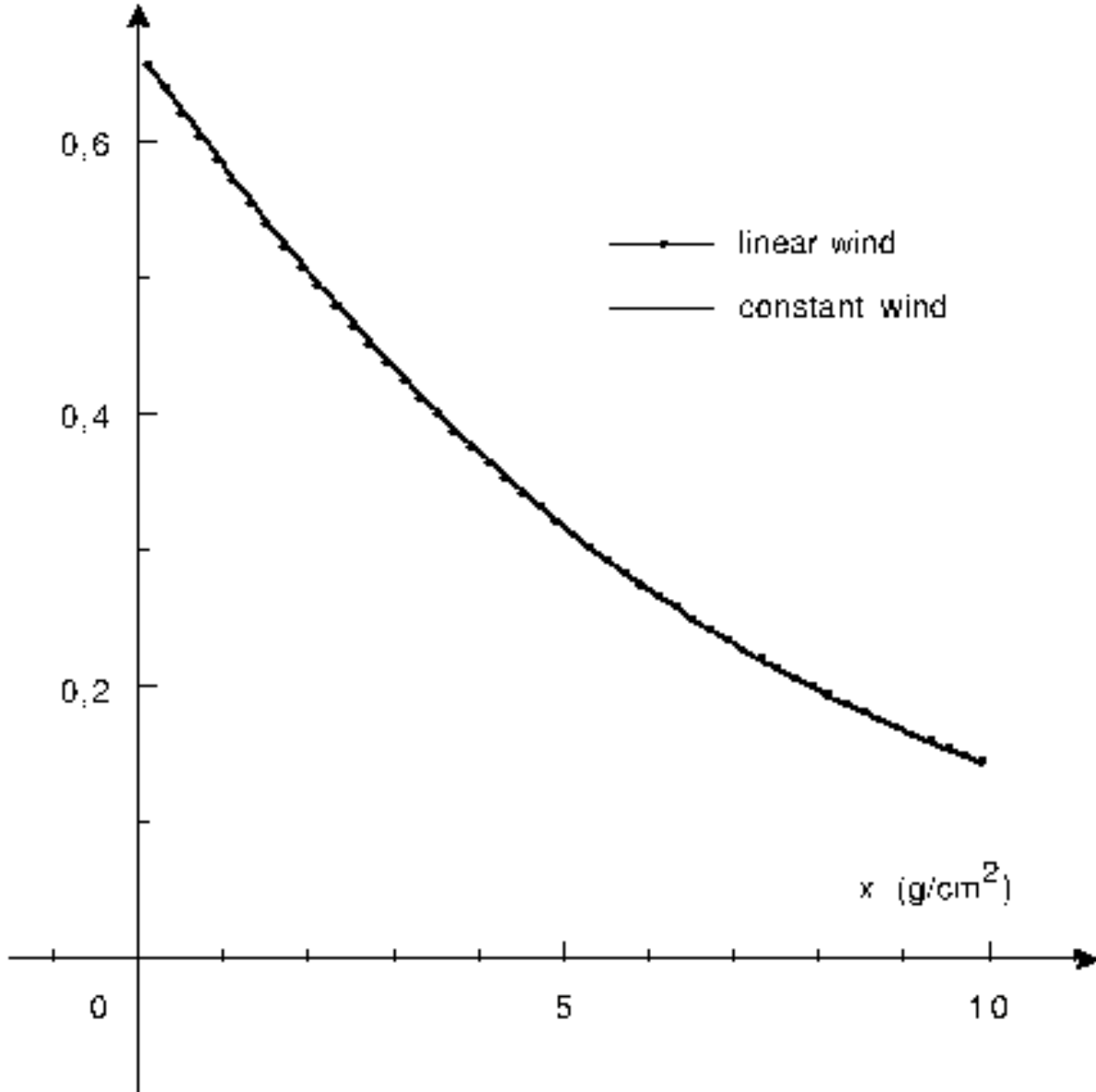


Fig. 6.— Path-length distributions for a linear (dots, $V_0 = 0.018 \text{ kpc Myr}^{-1} \text{ kpc}^{-1}$) and a discontinuous galactic wind (line, $V_c = 0.01 \text{ kpc Myr}^{-1}$). It appears that the effect of a linear or discontinuous wind are very similar. For each value of V_0 , it is possible to find a value of V_c yielding a grammage distribution which is very similar, with an accuracy better than one percent.

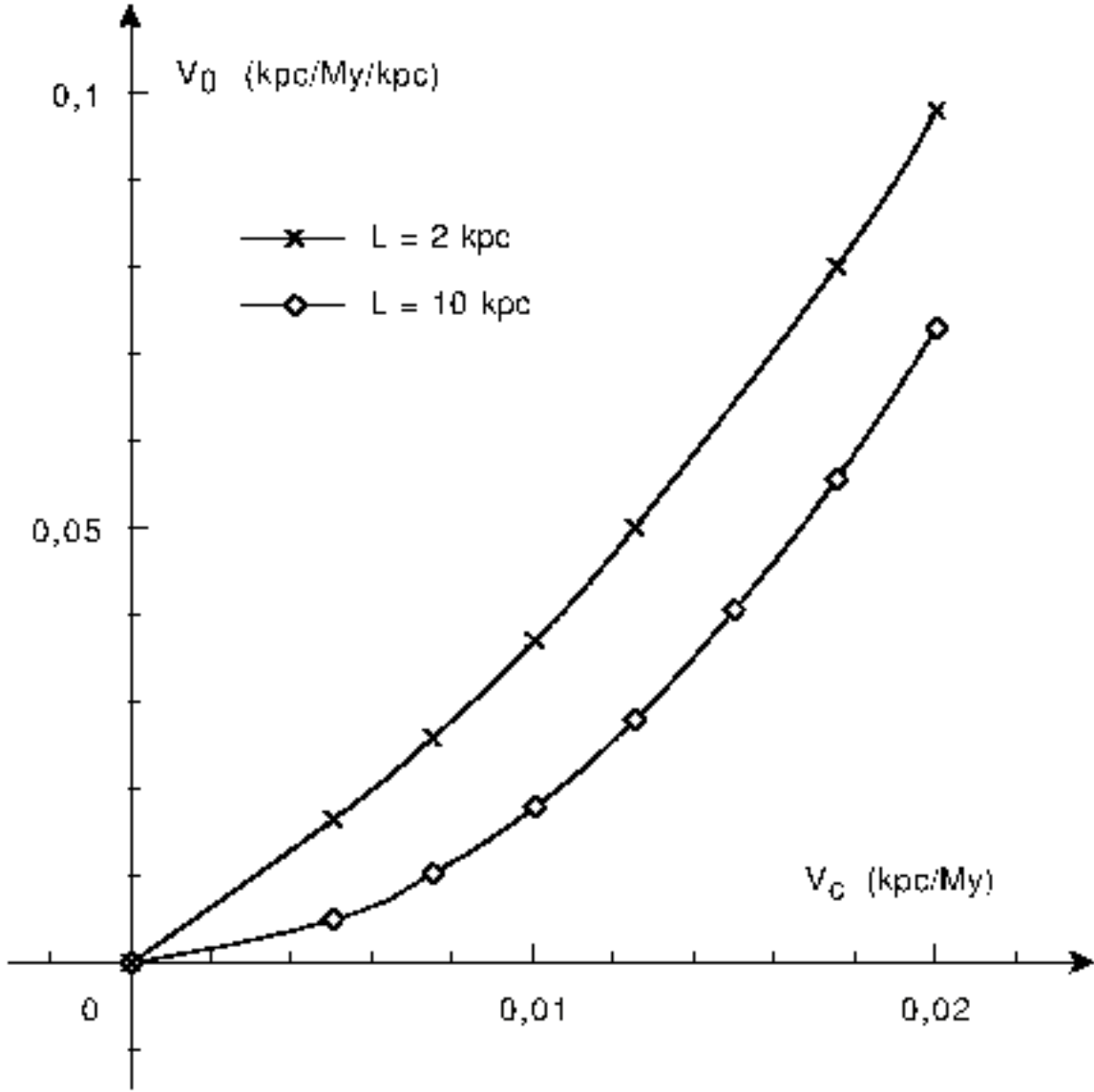


Fig. 7.— Correspondence between these the values of V_c (constant wind) and V_0 (linear wind) giving approximately the same path-length distributions, for two values of L .

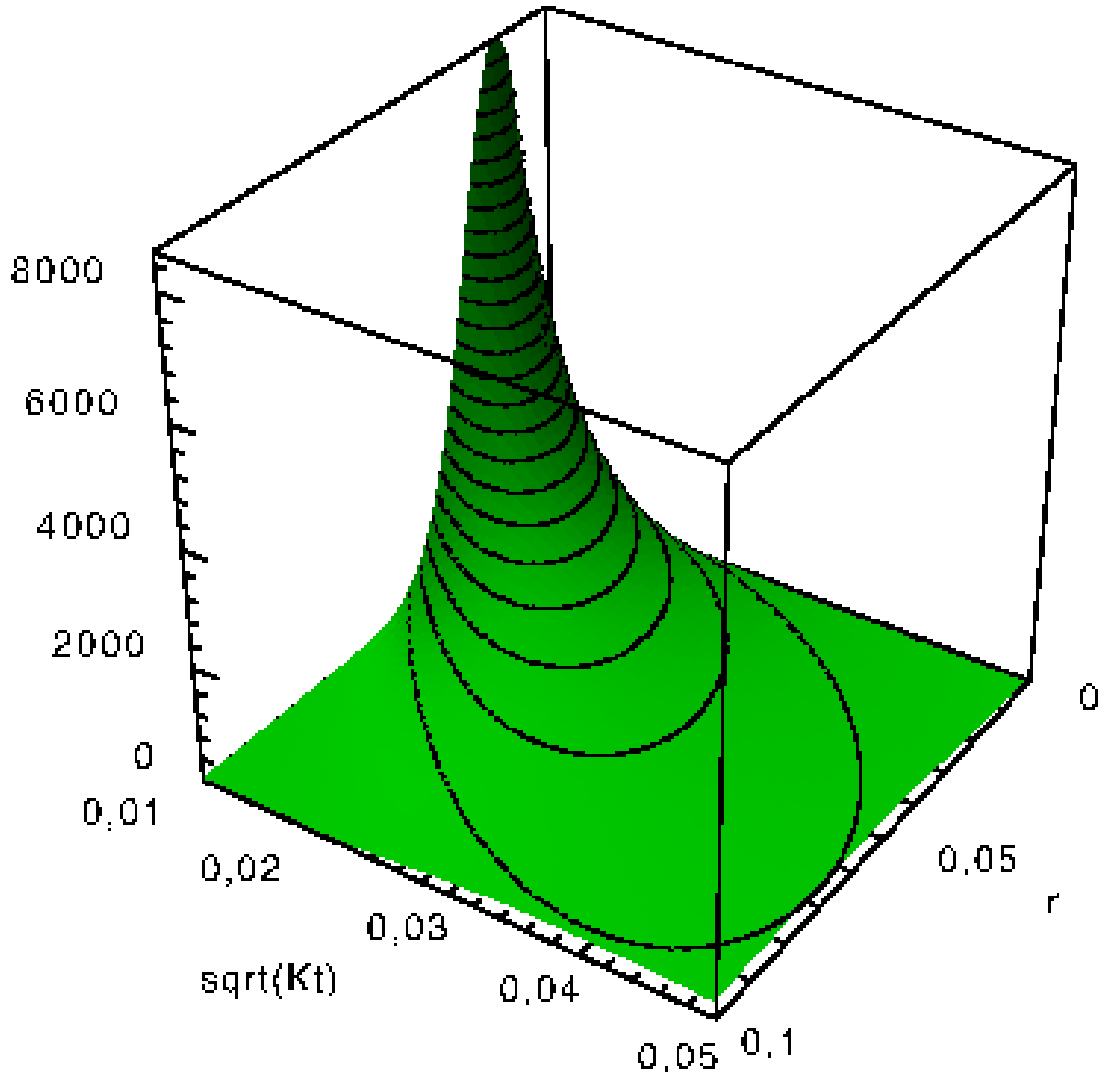


Fig. 8.— Contribution to the flux from a source ring located at a distance r and of age t , as a function of r and \sqrt{Kt} , in the case of pure diffusion, i.e. as given by $2\pi r\mathcal{N} \propto 2\pi r \exp(-r^2/4Kt)/(4\pi Kt)^{3/2}$. Numbers are in kpc.

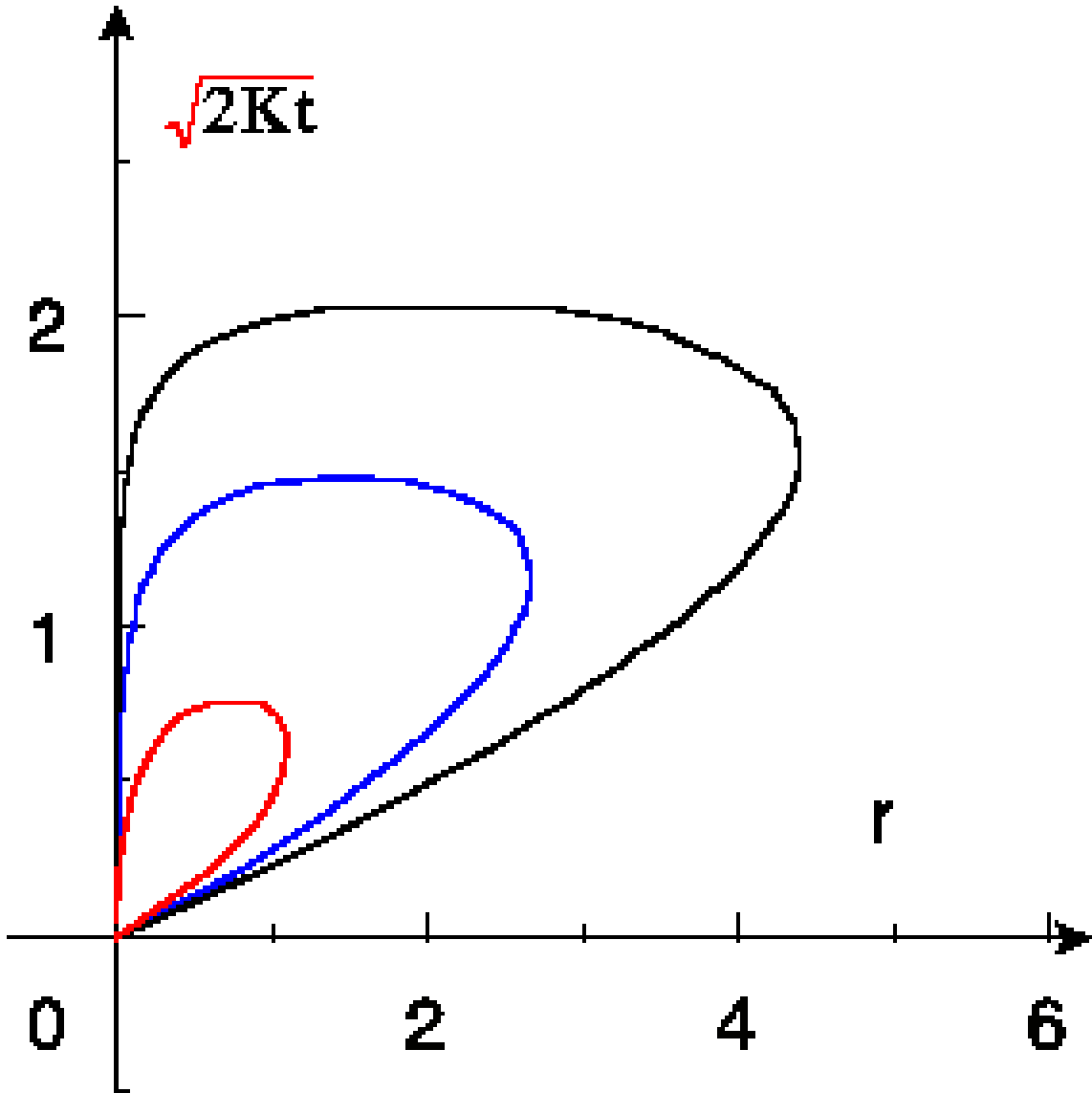


Fig. 9.— The regions of the $(r, \sqrt{2Kt})$ plane contributing for 50 % (inner curve), 90 % (middle curve) and 99 % (outer curve) of the flux are displayed, taking into account the escape through a boundary located at $L = 1$ kpc. Numbers on the axes are in kpc and a value $K = 0.03 \text{ kpc}^2 \text{ Myr}^{-1}$ has been assumed.

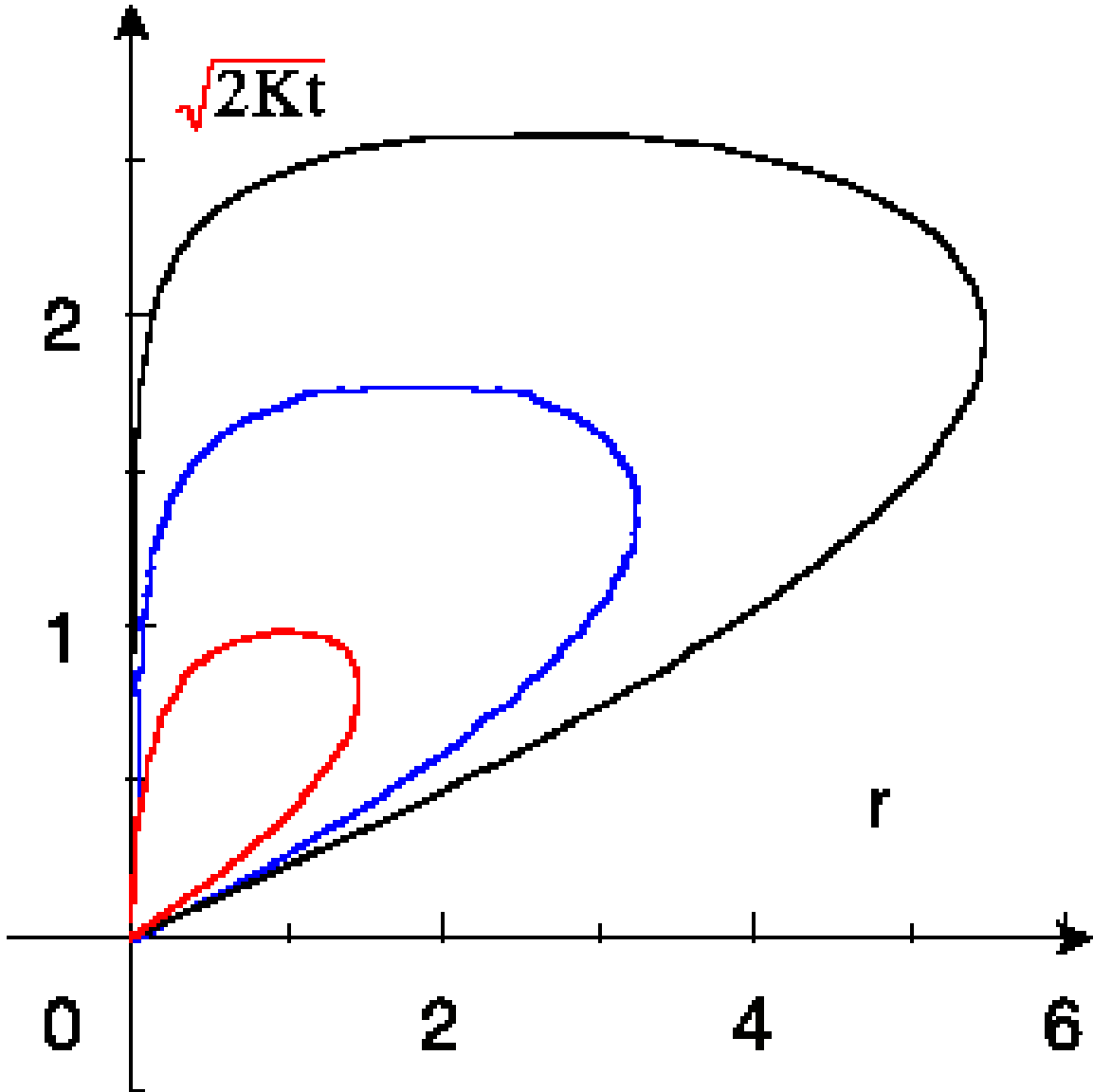


Fig. 10.— The regions of the $(r, \sqrt{2Kt})$ plane contributing for 50 % (inner curve), 90 % (middle curve) and 99 % (outer curve) of the flux are displayed, taking into account a convective wind with $r_w = 1$ kpc. Numbers on the axes are in kpc and a value $K = 0.03$ $\text{kpc}^2 \text{Myr}^{-1}$ has been assumed.

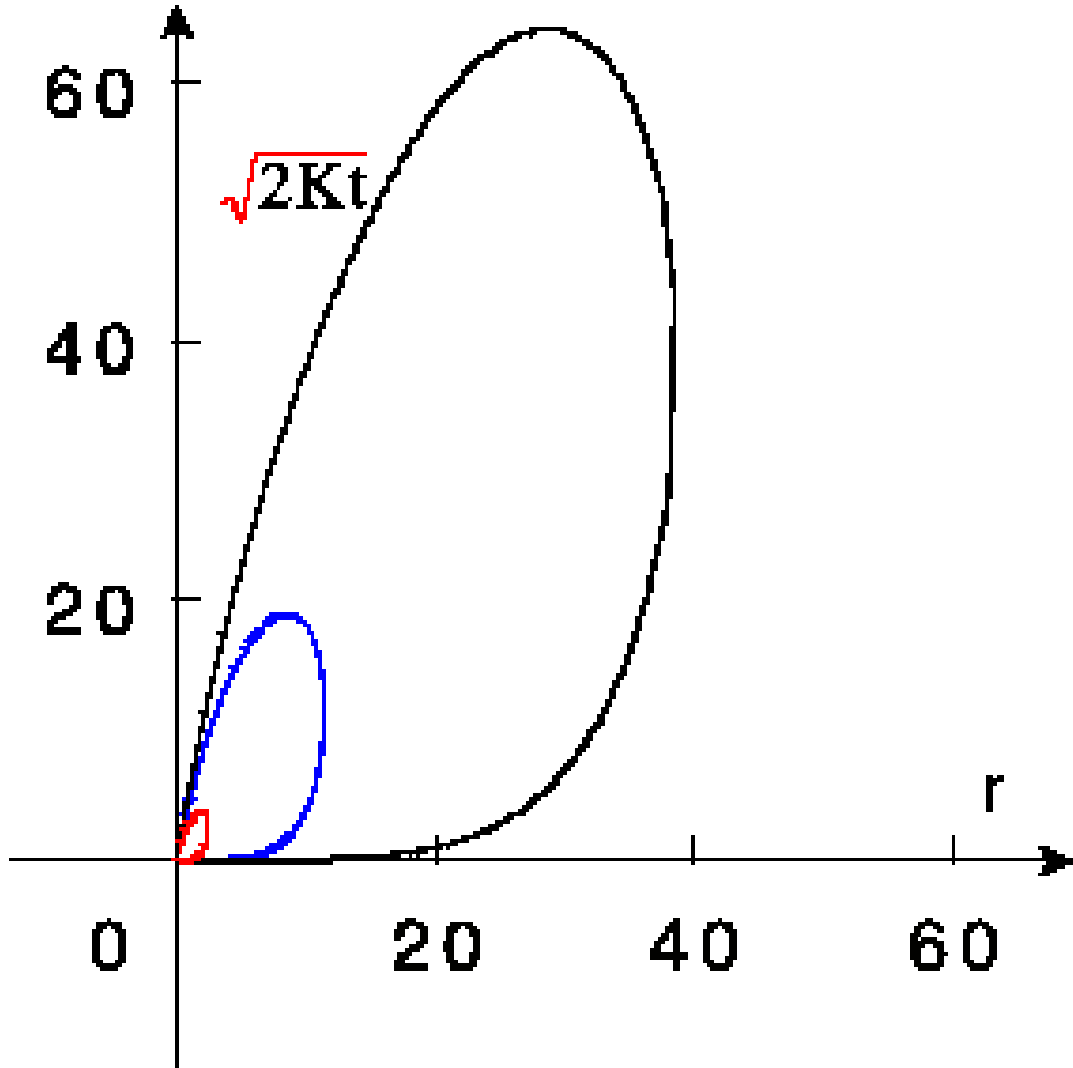


Fig. 11.— The regions of the $(r, \sqrt{2Kt})$ plane contributing for 50 % (inner curve), 90 % (middle curve) and 99 % (outer curve) of the flux are displayed, taking into account spallation with $r_{\text{spal}} = 1$ kpc. Numbers on the axes are in kpc and a value $K = 0.03$ kpc² Myr⁻¹ has been assumed.